Barcelona Supercomputing Center
Centro Nacional de Supercomputación

EXCELENCIA SEVERO OCHOA

Exploring linkages between AMOC and ITCZ variability:

a tale of energy and momentum, of water and dust

Eduardo Moreno-Chamarro
John Marshall, David McGee
Tom Delworth, Brian Green, Eric Galbraith

MPI-M Joint Seminar
August 6, 2019
eduardo.moreno@bsc.es

Southward ITCZ shift during cold stadials (weak AMOC or collapse)

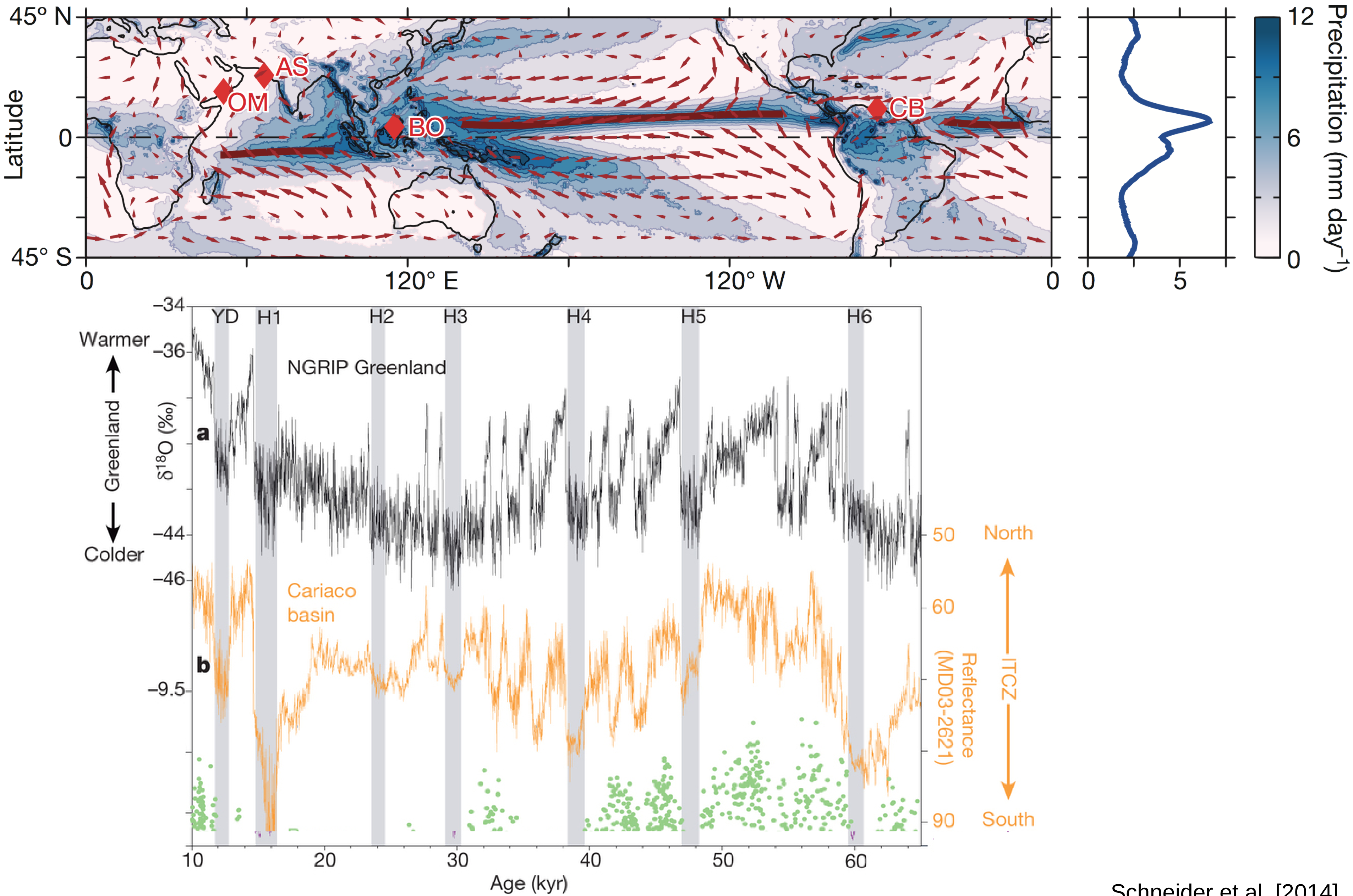

Schneider et al. [2014]

Southward ITCZ shift in a simulated AMOC collapse

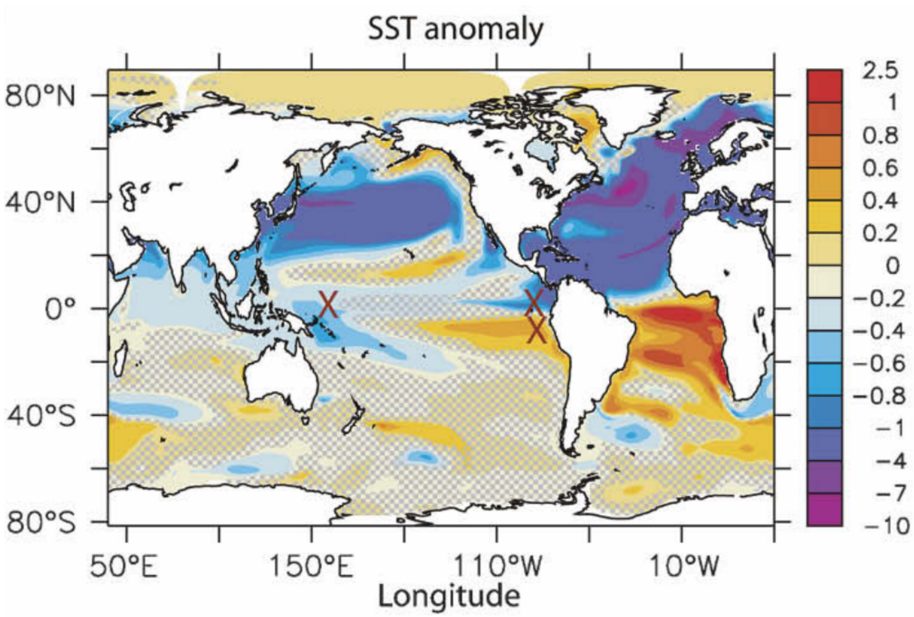

1. Freshwater flux in the North Atlantic
2. AMOC collapse
3. North Atlantic SST and NH atmospheric cooling
4. Interhemispheric heating imbalance
5. Southward Hadley cell and ITCZ shift

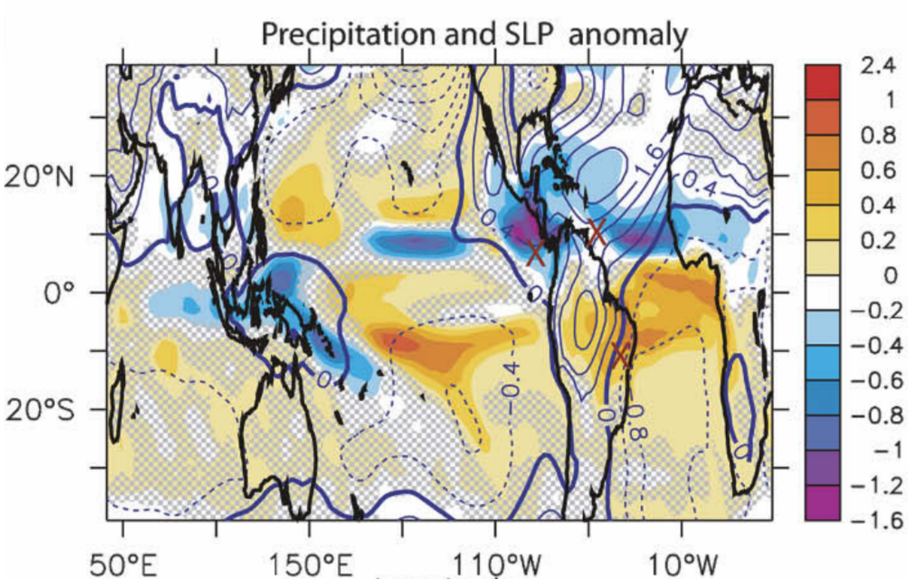

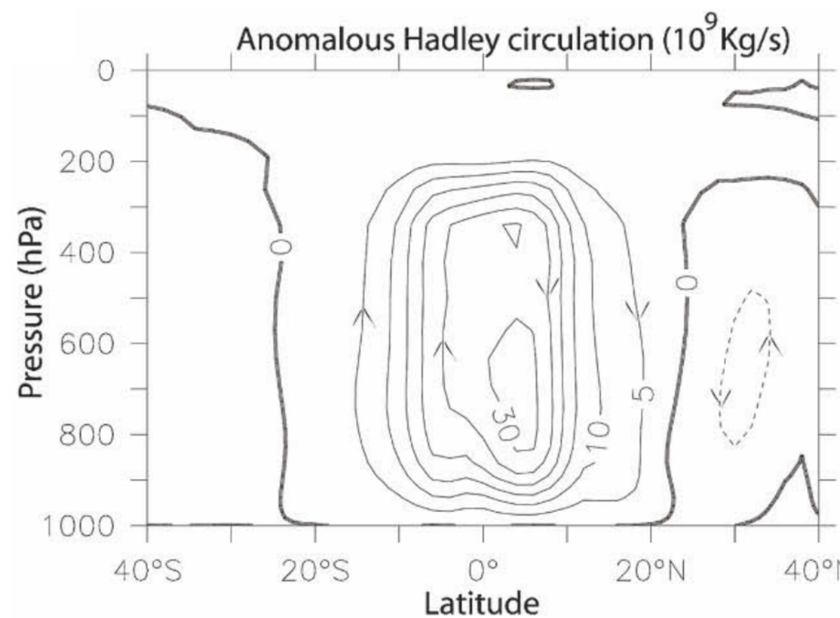

Zhang and Delworth [2005]

Link between the AMV and ITCZ variability in observations

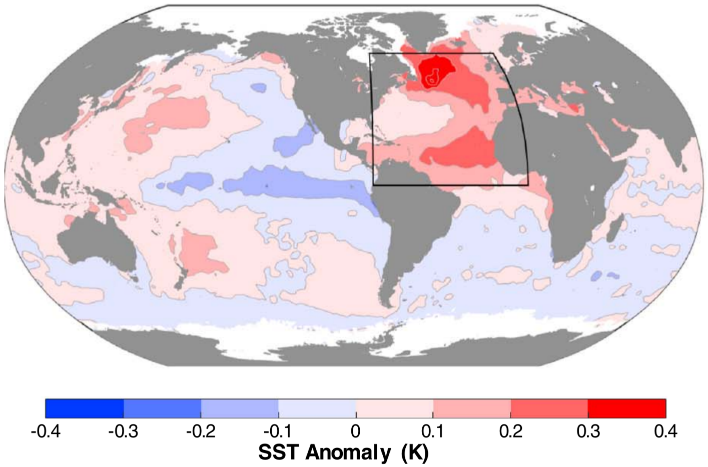

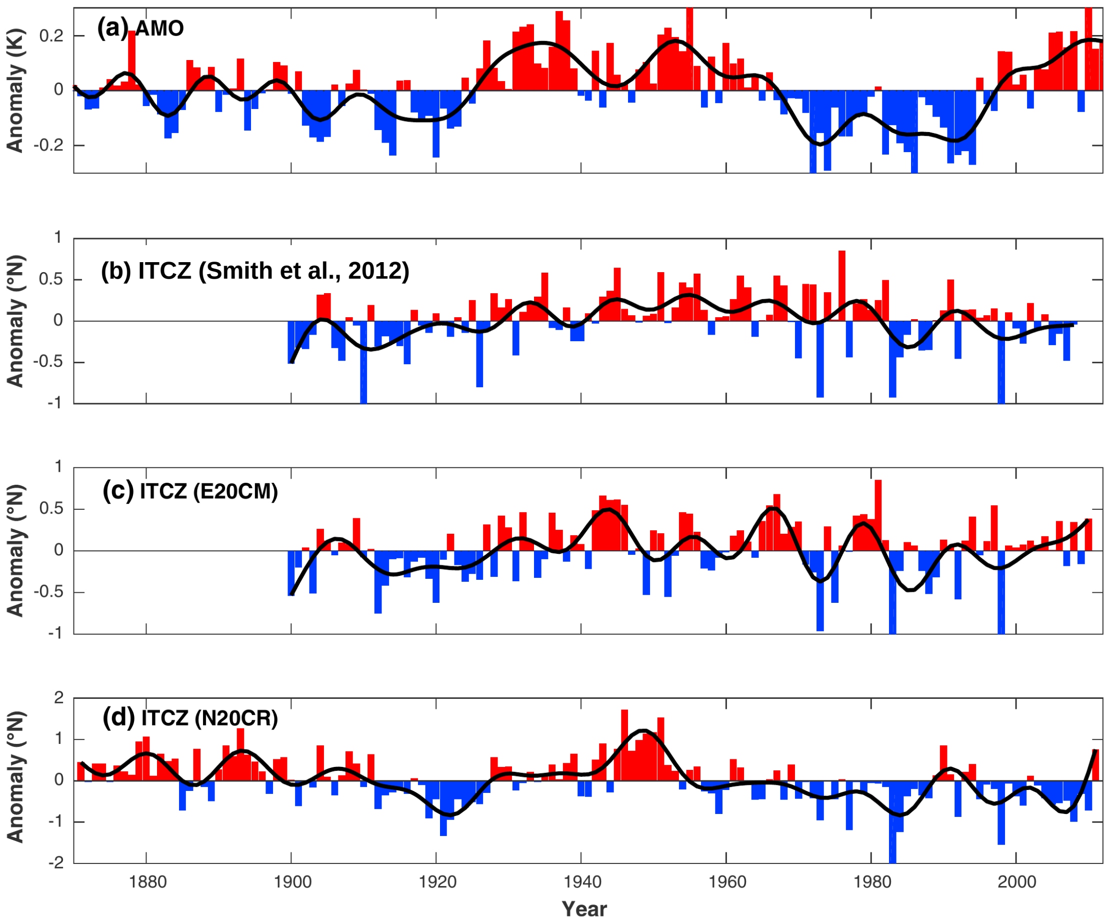

Green and Marshall [2017]

Links between the AMV and PDO and ITCZ variability in observations

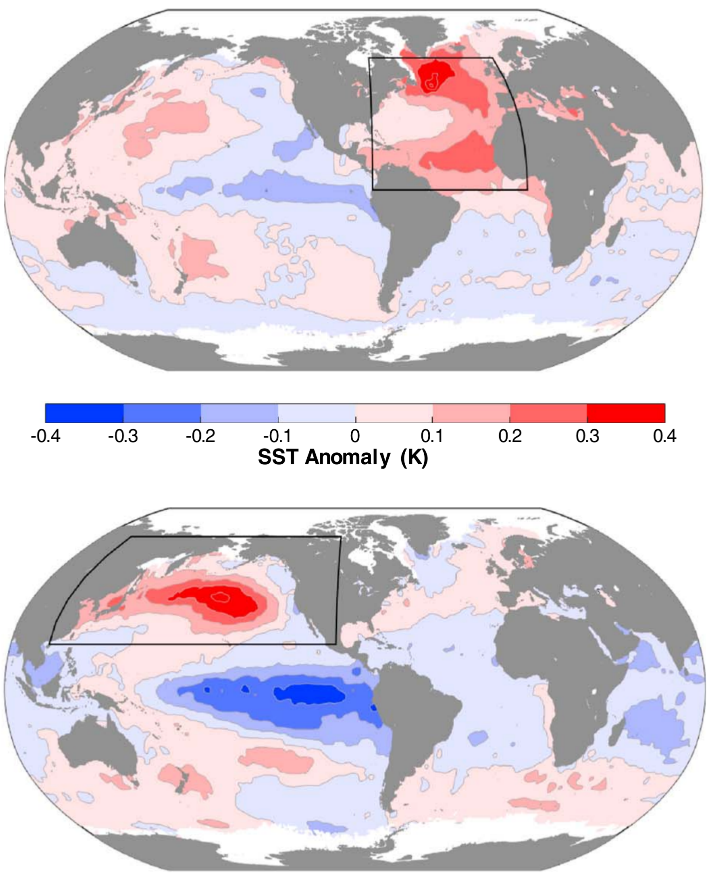

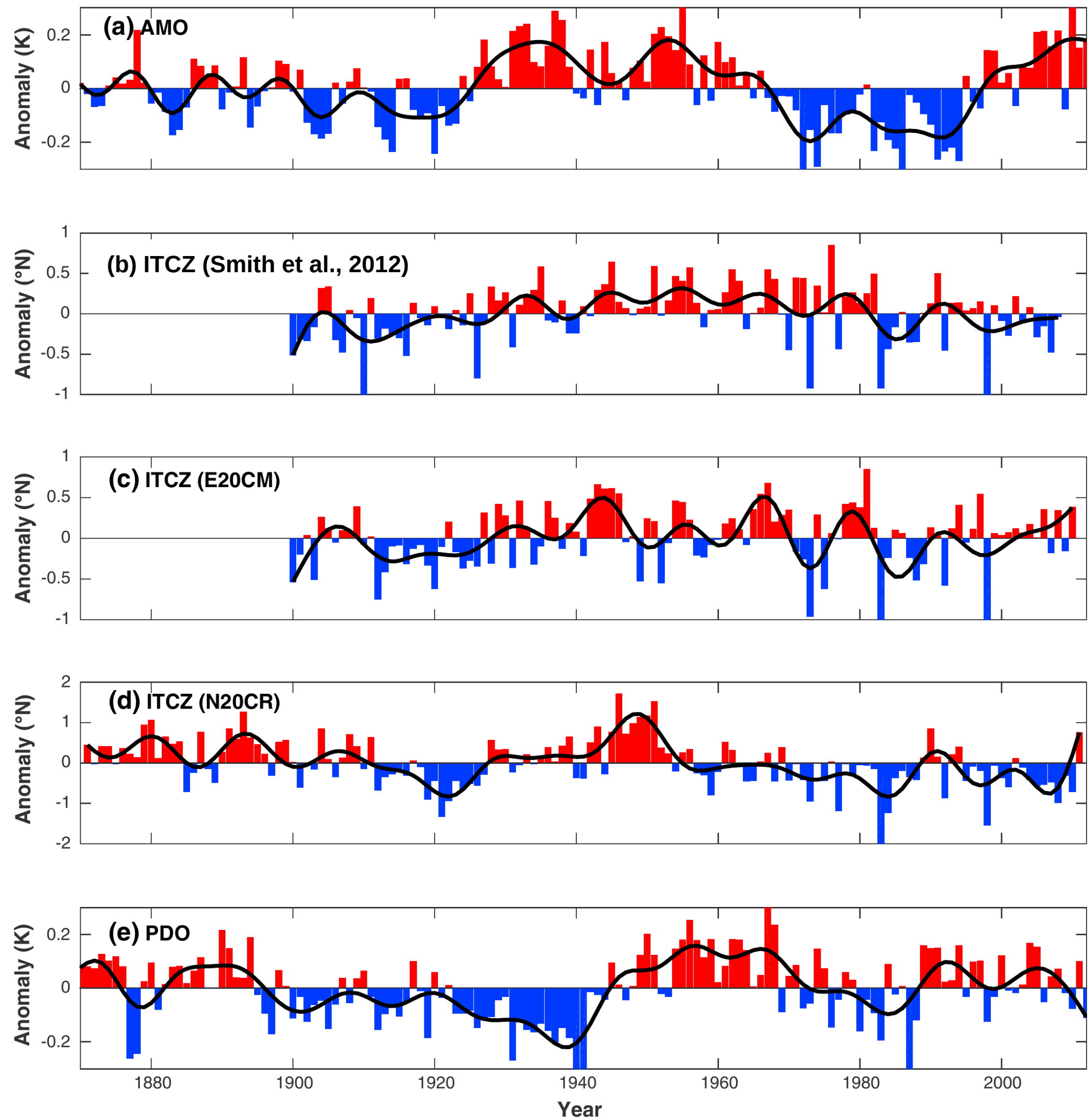

Green and Marshall [2017]

1. Inadequate observational record to extend observed AMV–ITCZ link to the AMOC
   Can such a link be made?

2. Tenuous ITCZ–PDO link in observations
   Can it be confirmed?

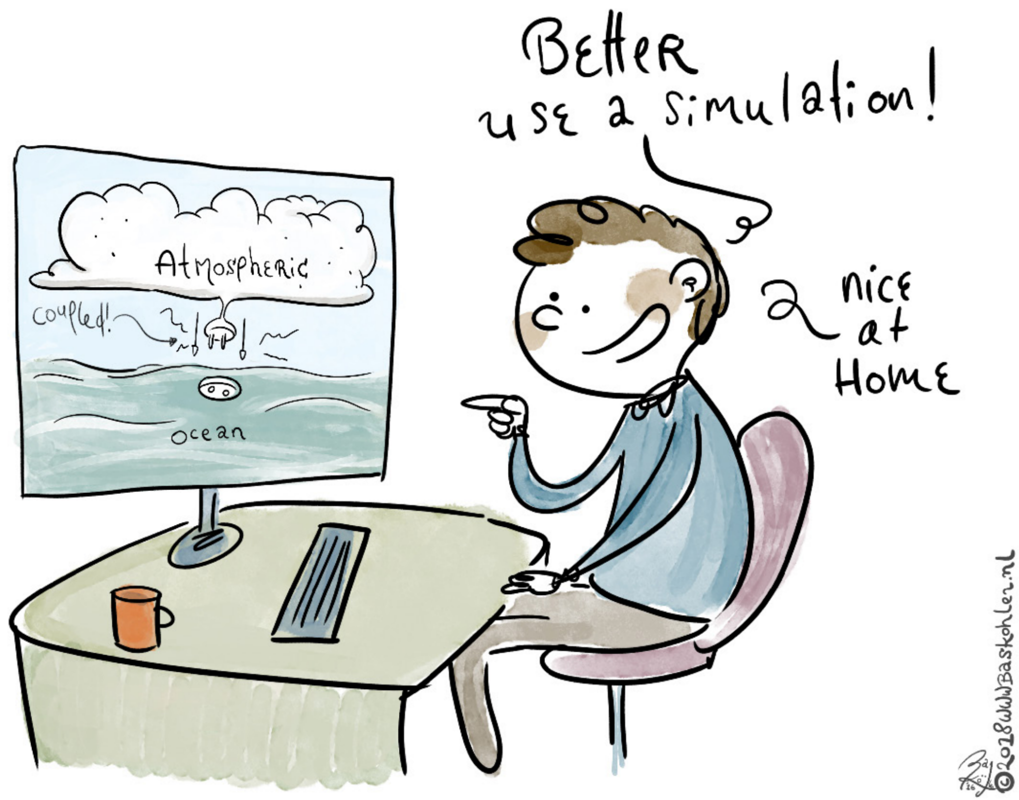

Simulations with the GFDL's CM2.1 coupled climate model

→ 4000-year-long control:
  1860's forcing

→ 10-member ensemble:
  Winter NAO-derived heat flux anomaly
  No net heating/cooling to the system
  50-year-long sinusoidal 1stdv amplitude

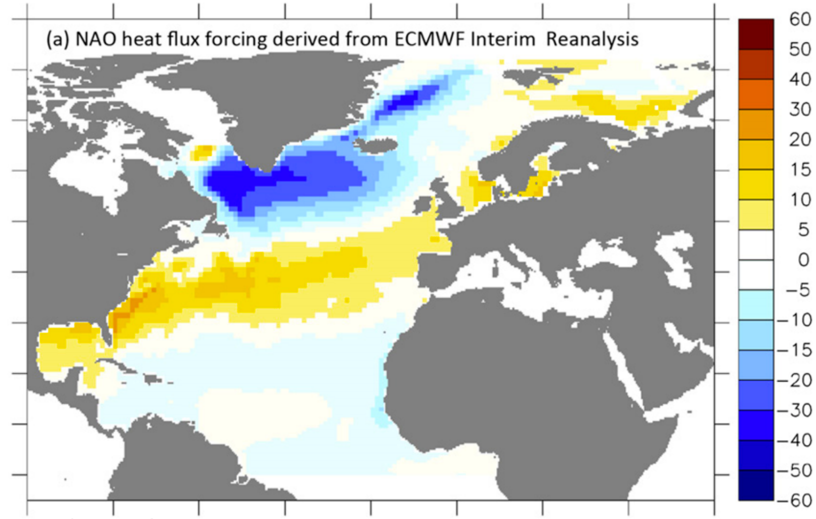

Delworth and Zeng [2015]

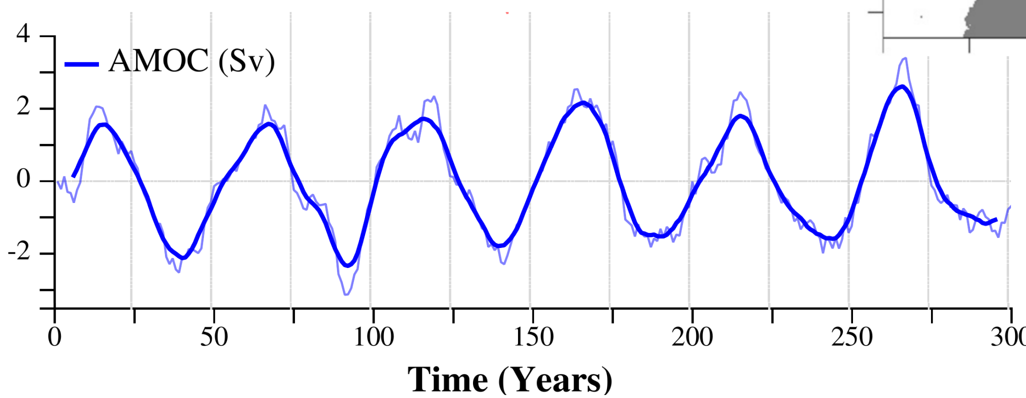

Moreno-Chamarro et al. [in review]

ITCZ position, AMV, and AMOC variability in the forced ensemble

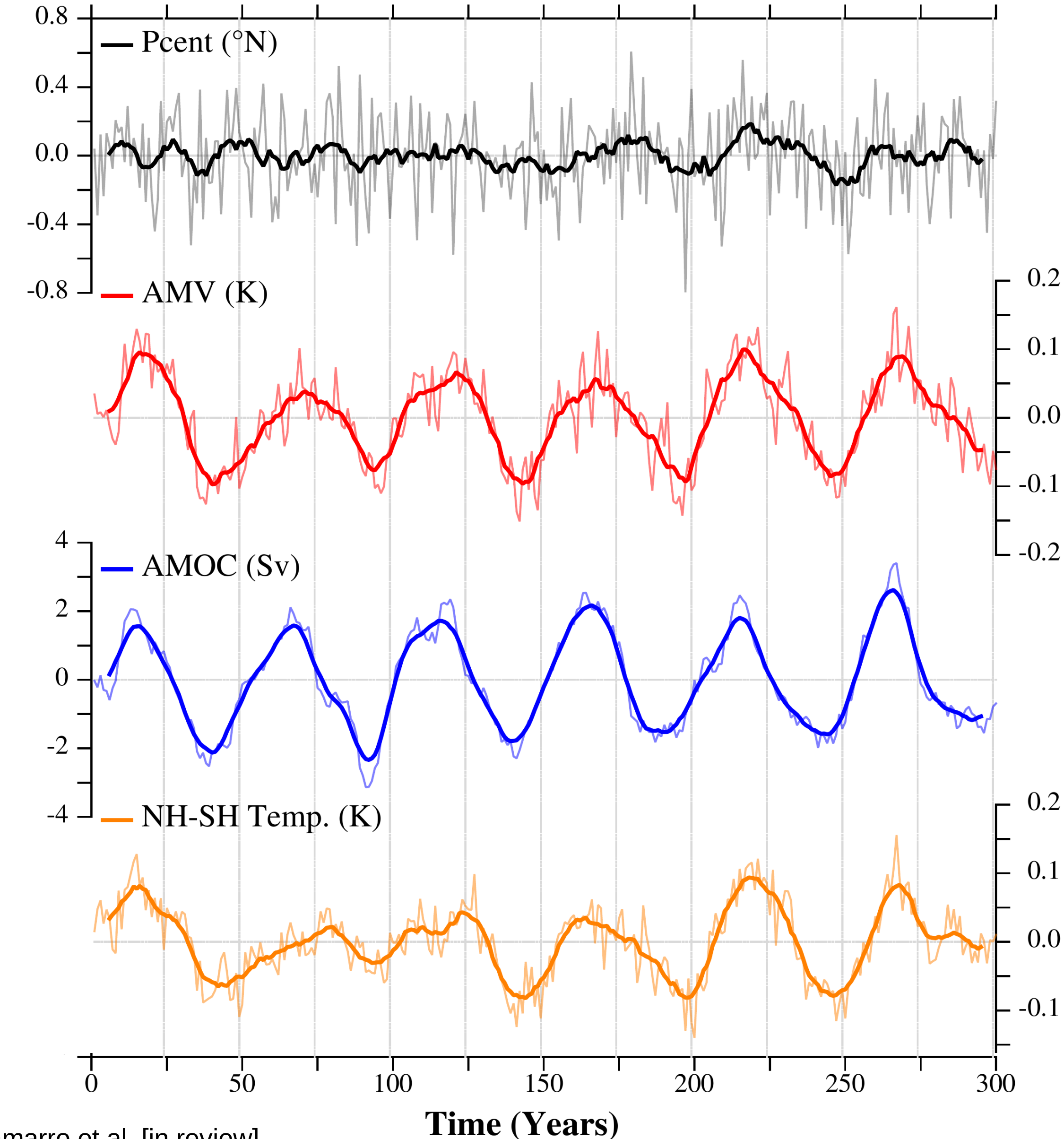

Moreno-Chamarro et al. [in review]

ITCZ position, AMV, and AMOC variability in the control

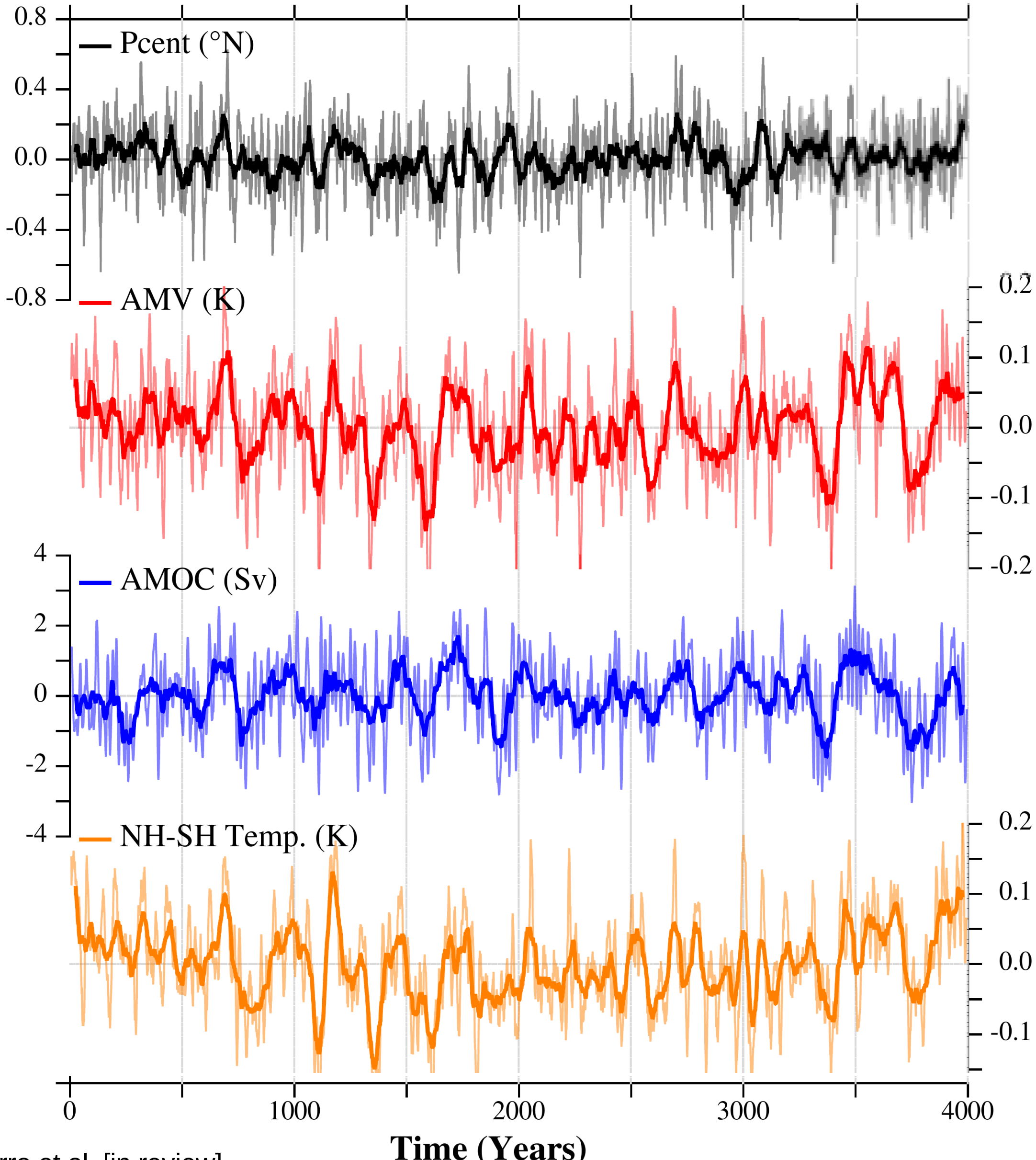

Moreno-Chamarro et al. [in review]

ITCZ–AMV–AMOC coherent variability

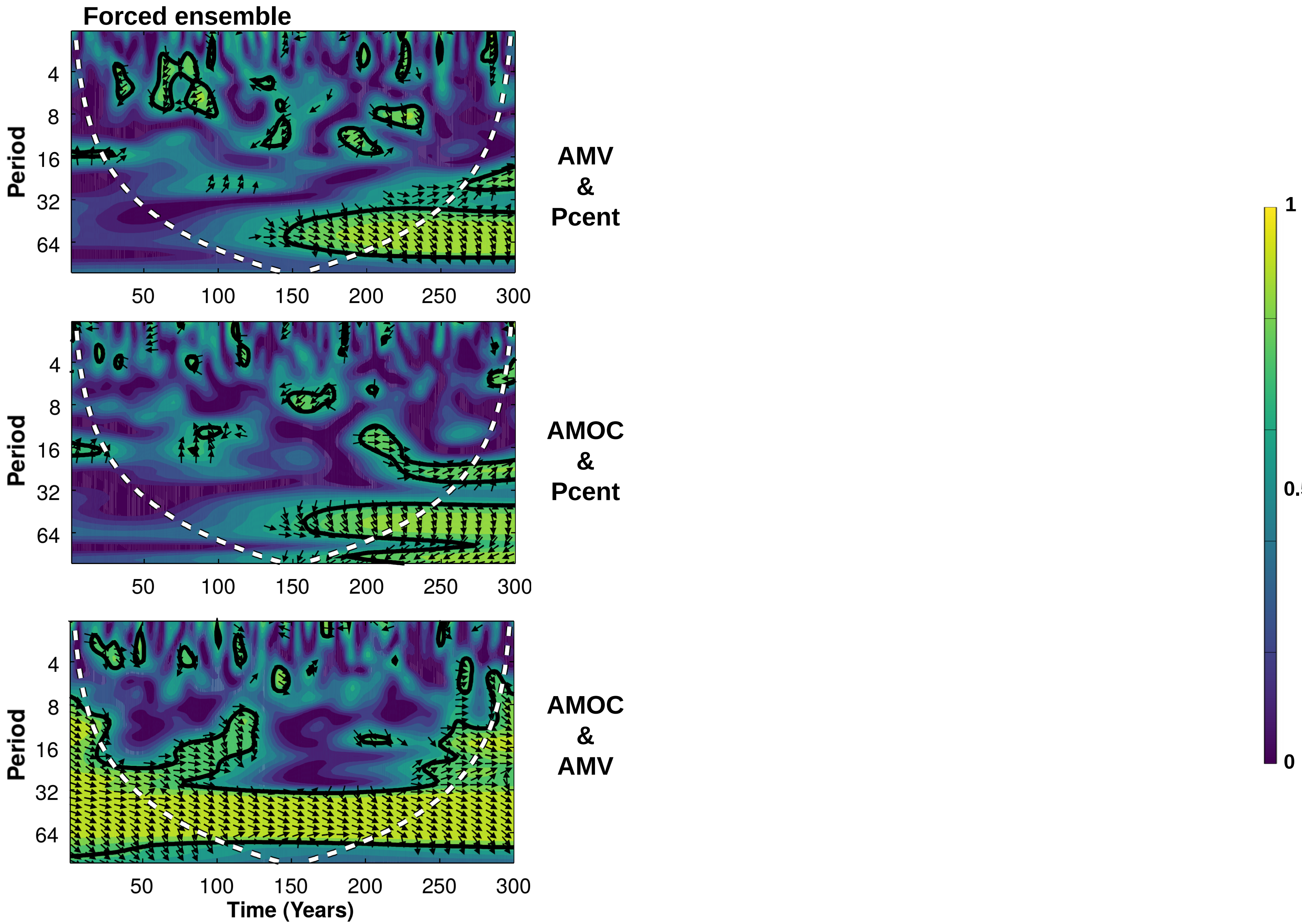

Moreno-Chamarro et al. [in review]

ITCZ–AMV–AMOC coherent variability

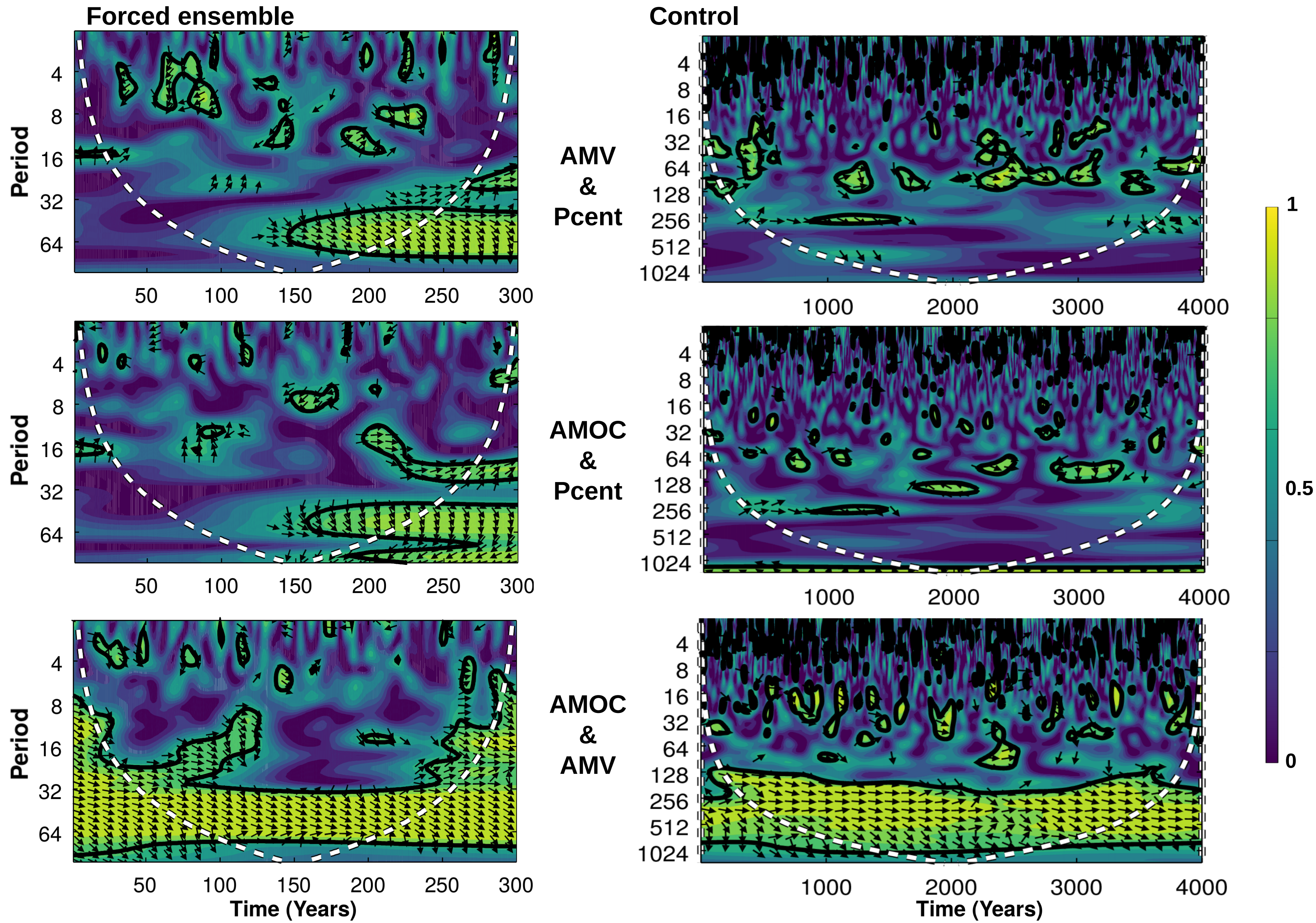

Moreno-Chamarro et al. [in review]

Anomalies between years above and below 1stdv in AMV

Anomalies: Precipitation (shading; mm/day) and 1000-hPa winds (arrows; m/s)
Model precipitation climatology (contours; mm/day)

Forced ensemble – Multidecadal time scales

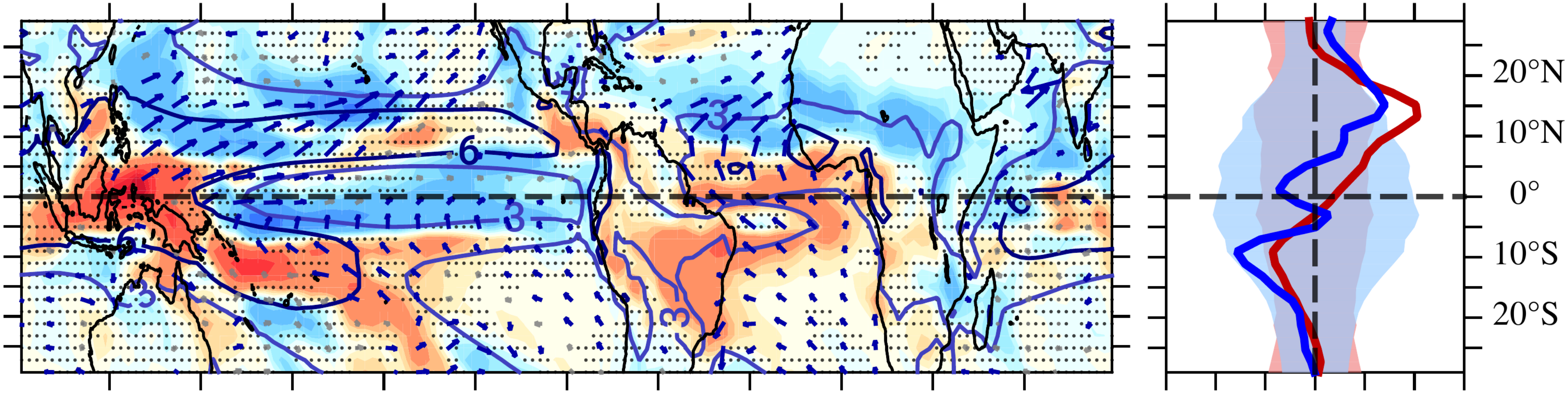

Control – Multicentennial time scales

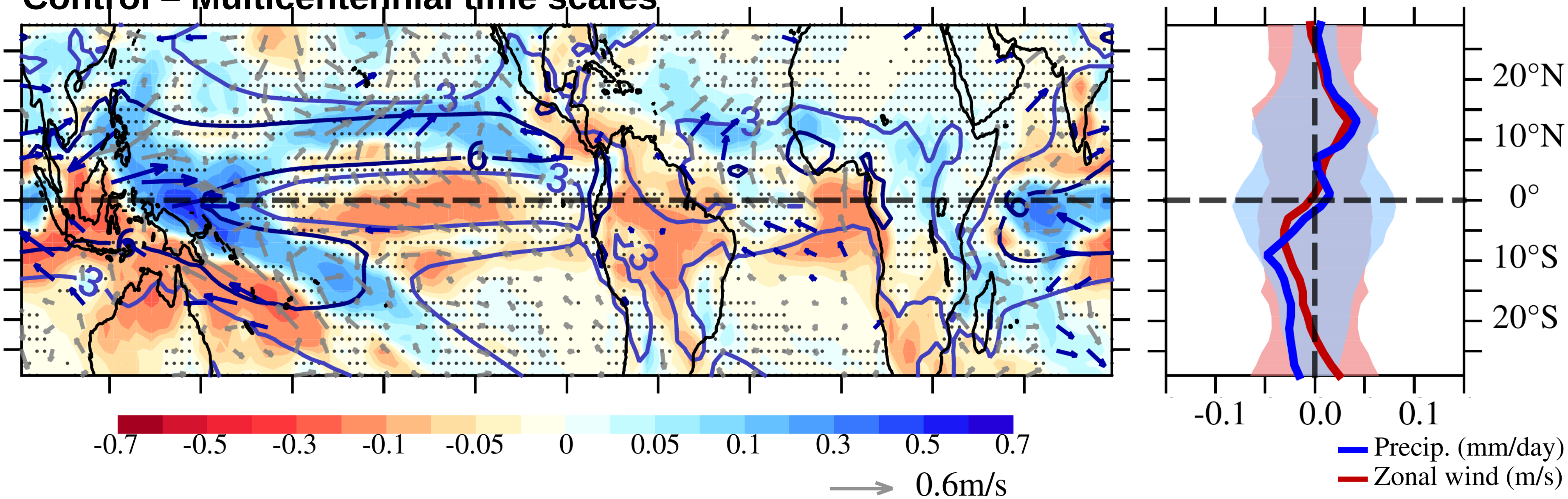

Anomalies between years above and below 1stdv in AMV

Anomalies in the zonally averaged asymmetric temperature (K)

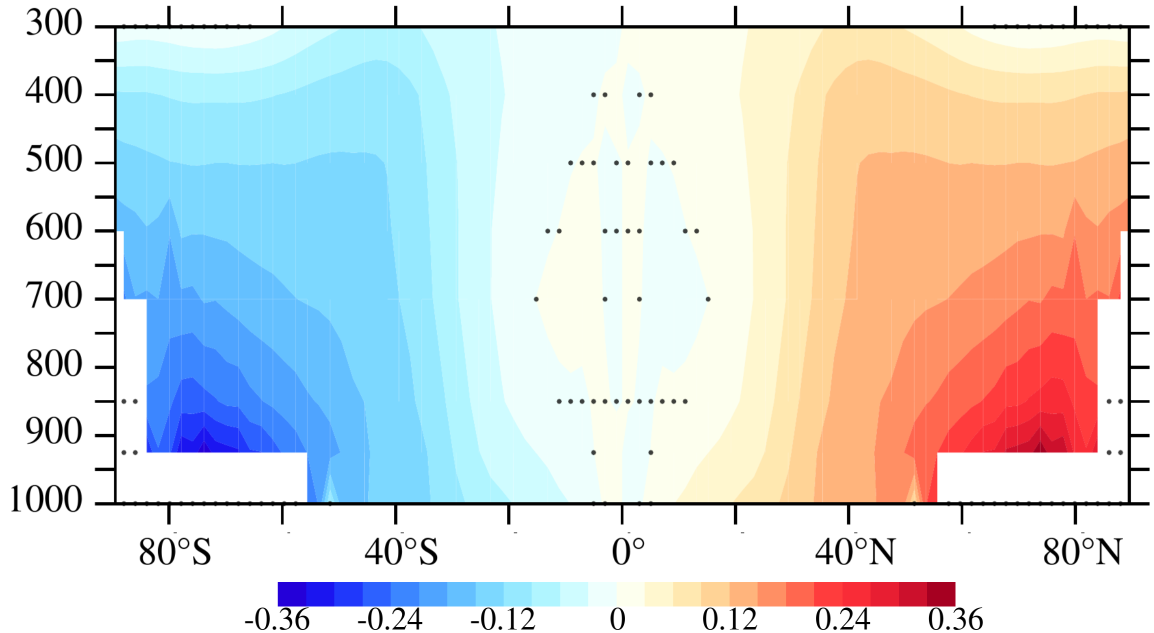

Anomalies in heat transports (PW)

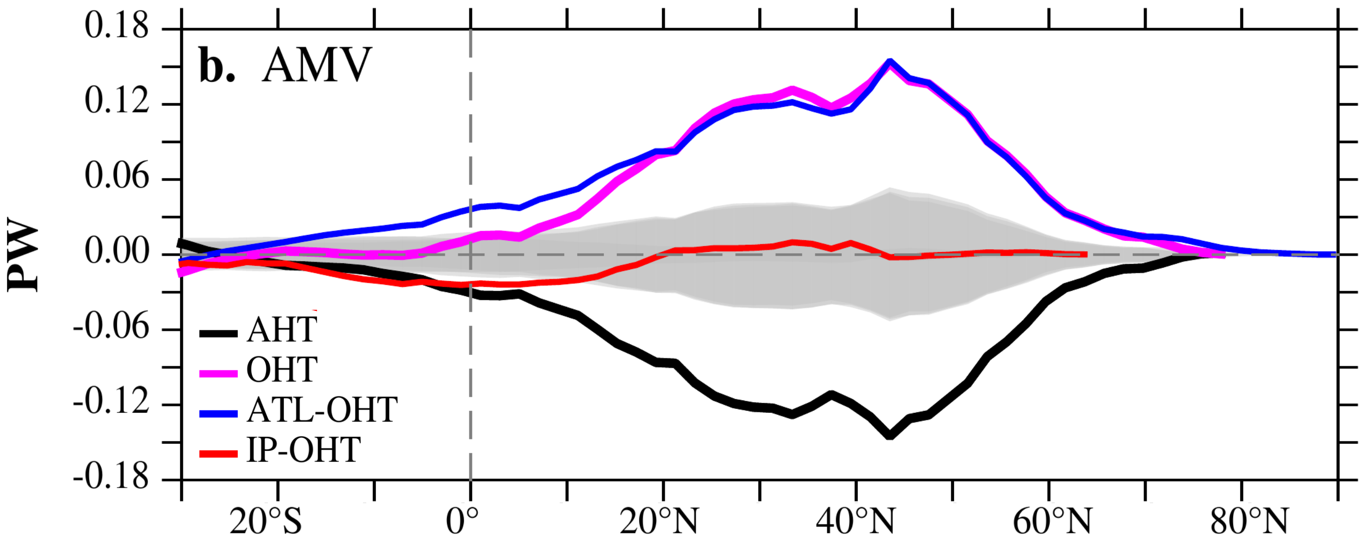

Moreno-Chamarro et al. [in review]

No coherent variability between the ITCZ position and PDO

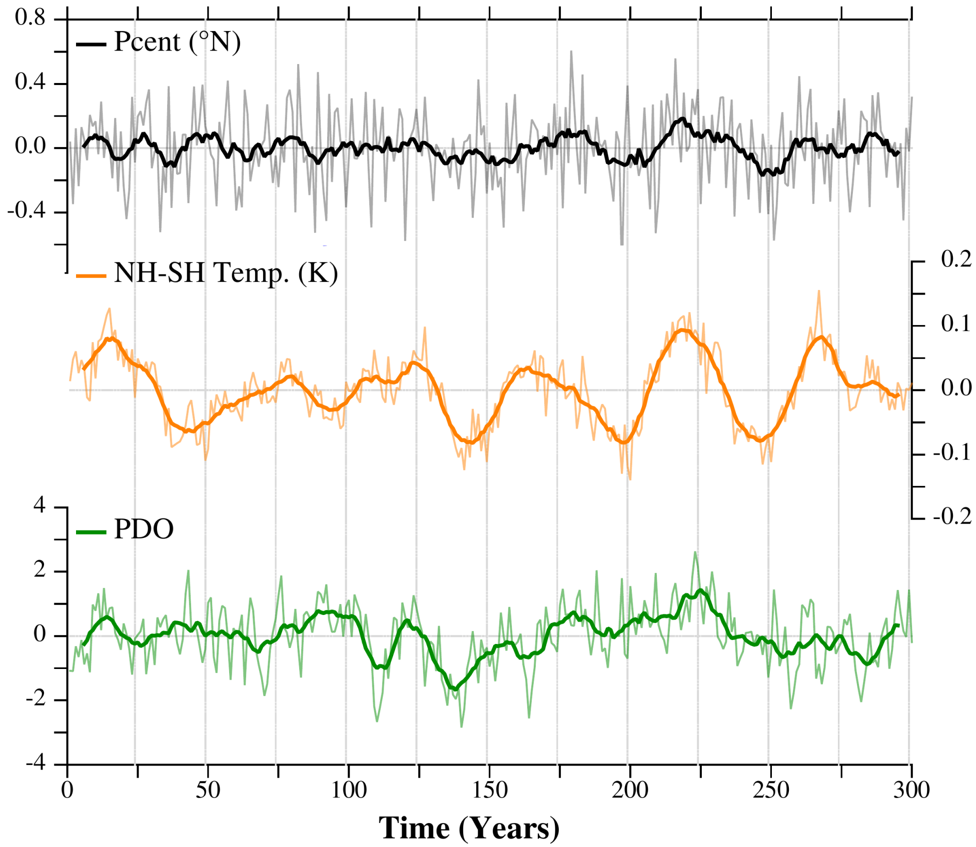

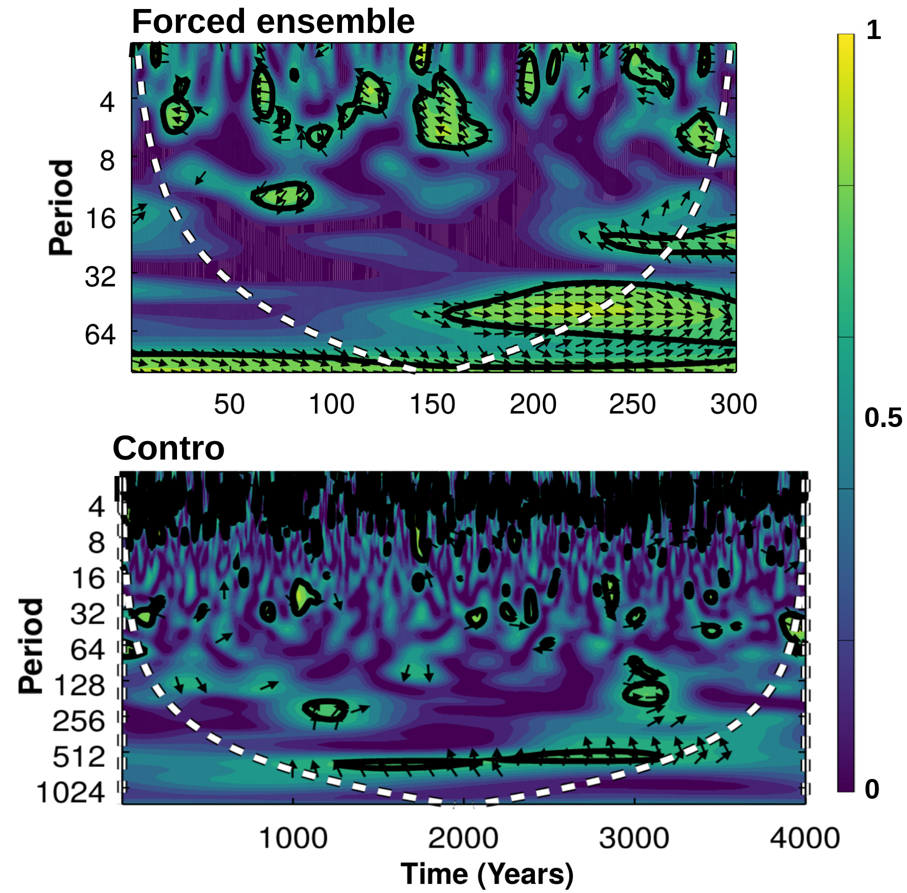

Moreno-Chamarro et al. [in review]

Anomalies between years above and below 1stdv in PDO

Anomalies: Precipitation (shading; mm/day) and 1000-hPa winds (arrows; m/s)
Model precipitation climatology (contours; mm/day)

Control

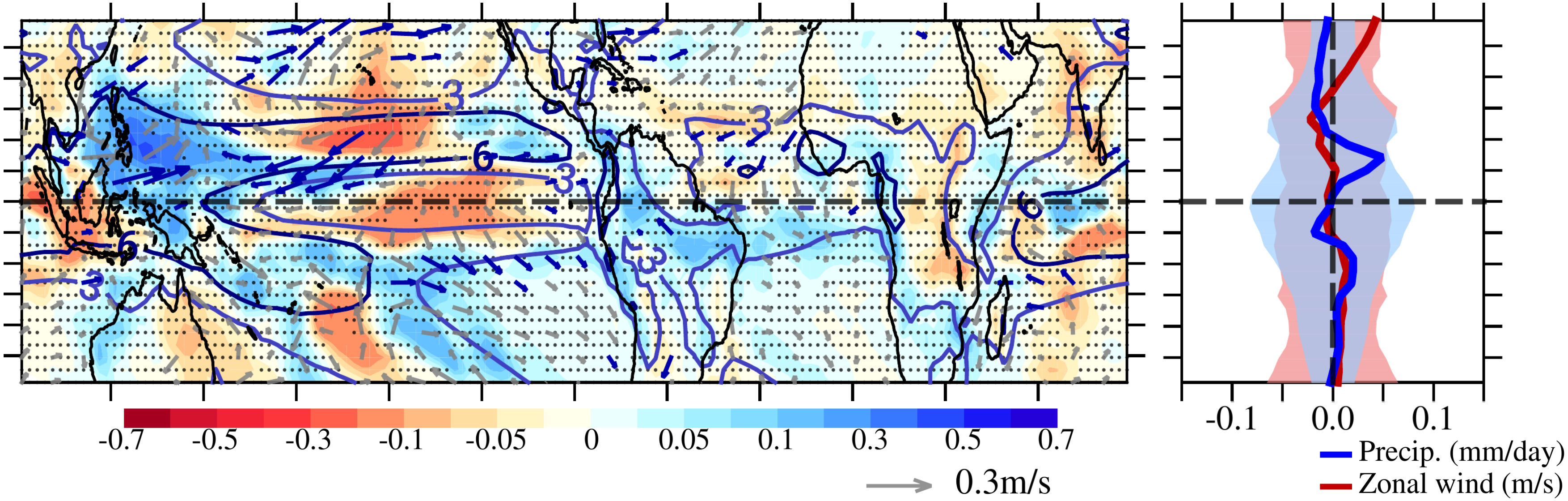

Anomalies in the zonally averaged asymmetric temperature (K)

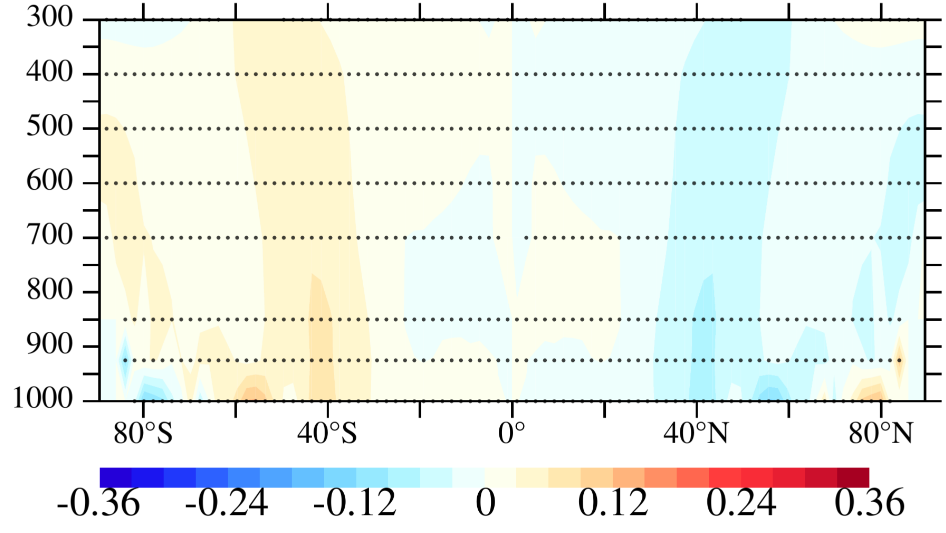

Summary: Linking ITCZ migrations to AMOC and North Atlantic/Pacific SST decadal variability

1. AMV phase change driven by AMOC's cross-equatorial OHT change forcing an atmospheric interhemispheric energy imbalance. This compensated by a meridional ITCZ shift

   – The link on decadal and multicentennial time scales in the forced ensemble and control respectively

   – Different regional precipitation anomalies for similar ITCZ shift

2. PDO not driving ITCZ migrations due to the former not modulating the interhemispheric energy balance

Southward ITCZ shift during cold stadials (weak AMOC or collapse)

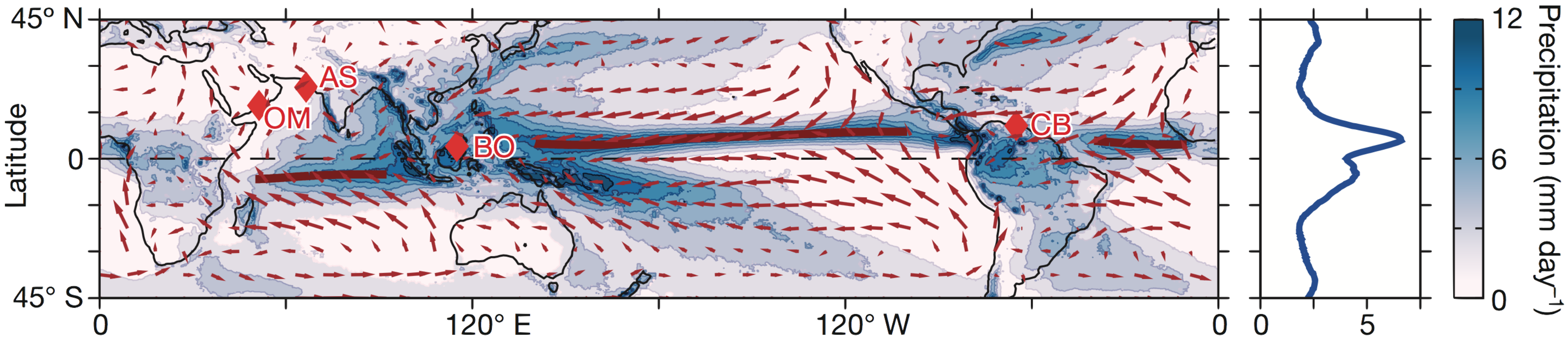

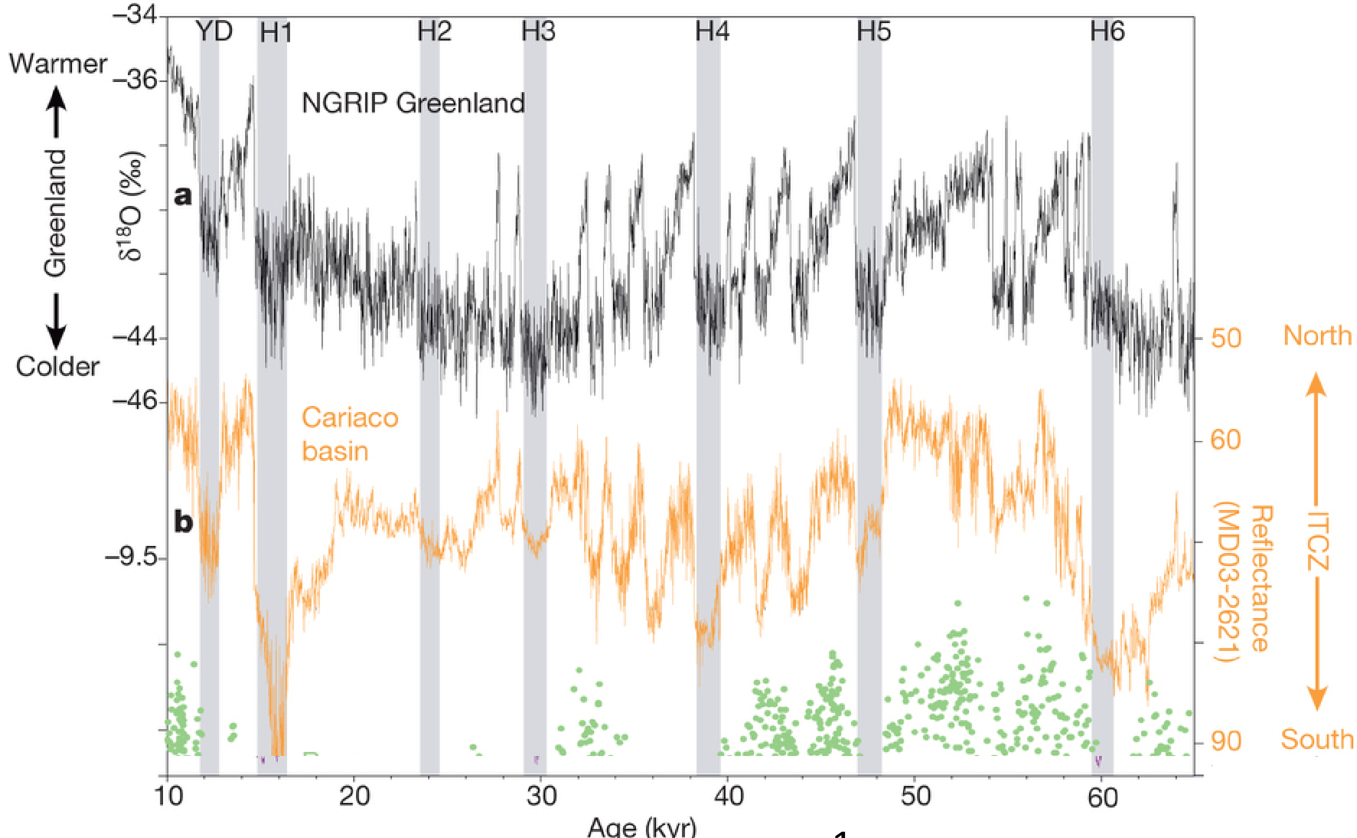

Schneider et al. [2014]

Simulated precipitation and surface wind anomalies during a southward ITCZ shift during an AMOC collapse

Why the shape in zonal wind anomalies? Can it be found in proxies?

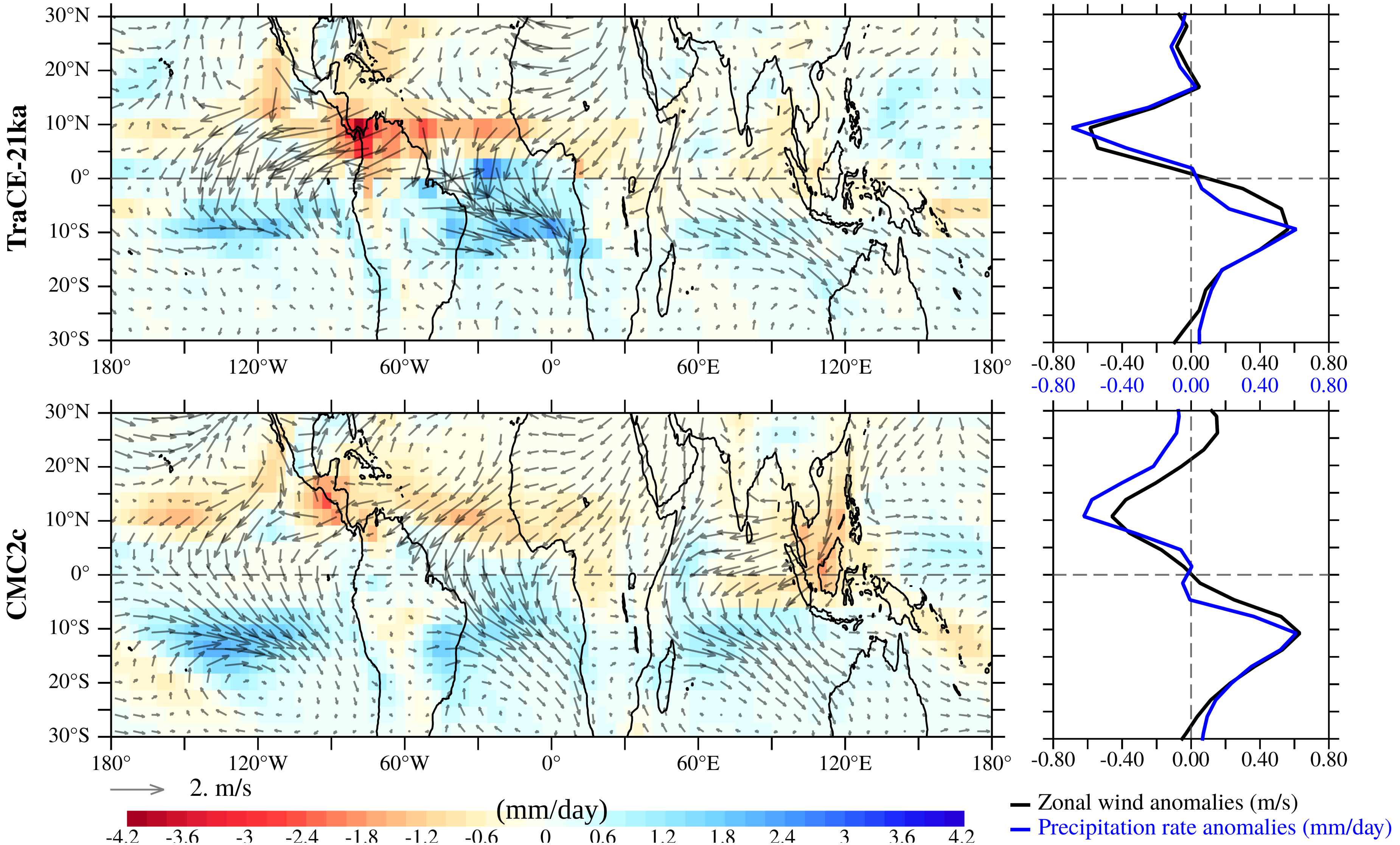

McGee et al. [2018]

Trade wind changes as fingerprint of a southward ITCZ and Hadley cell shift

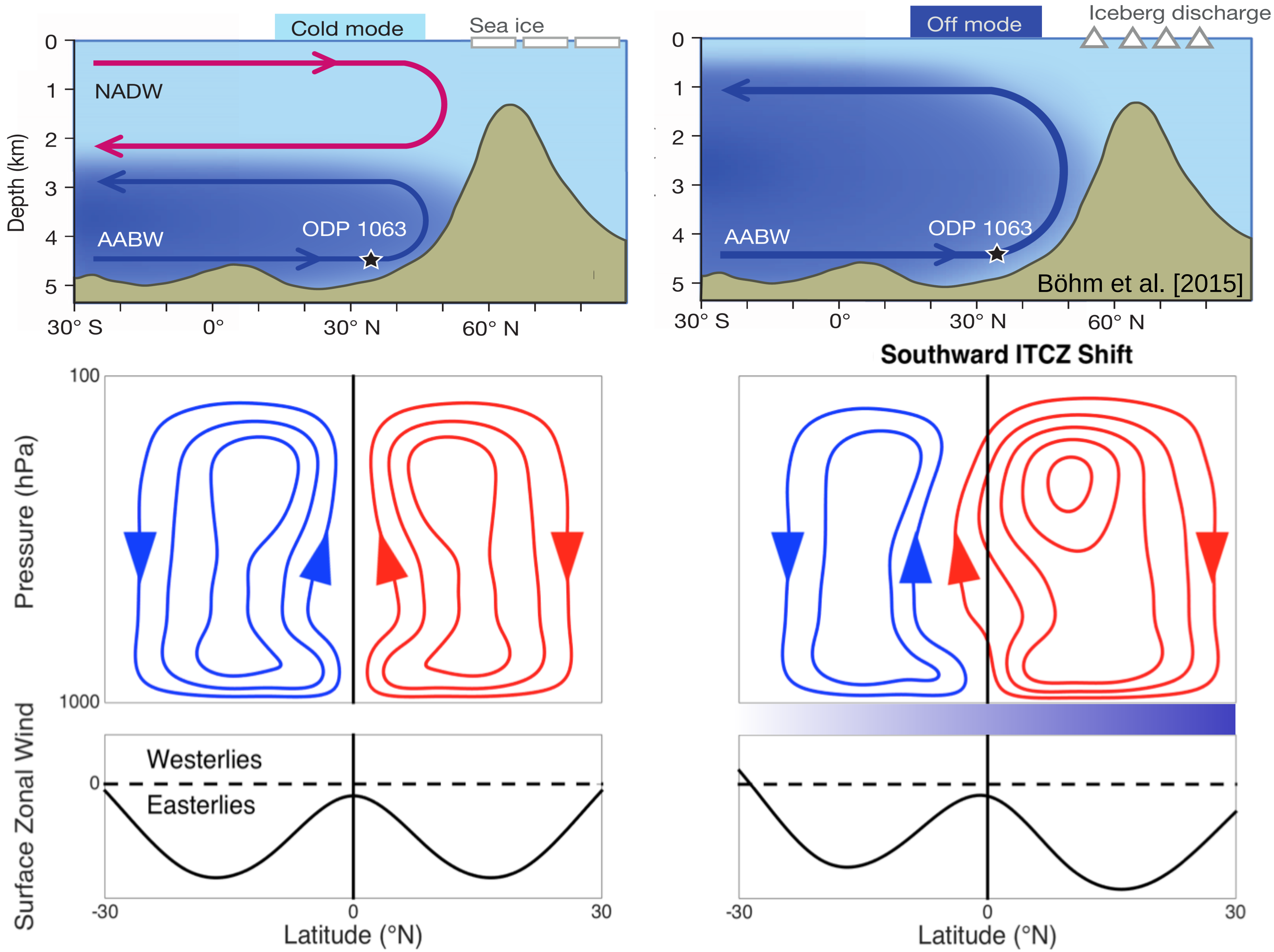

Proxies for trade wind changes during Heinrich stadials

– Windblown dust:
  Dust flux and grain size
  Sand dune activity

– Wind-driven coastal upwelling
  SST
  Nutrient supply (e.g., primary productivity, species distribution)

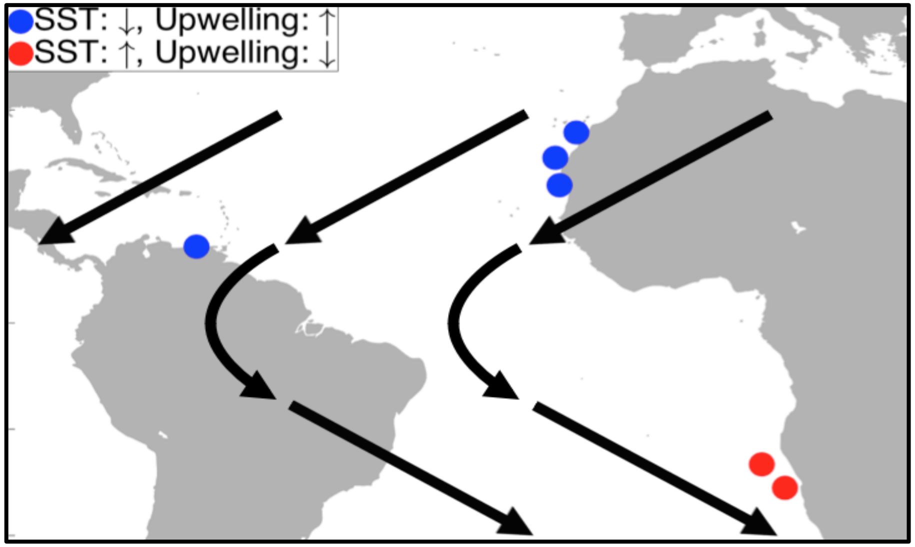

McGee et al. [2018]

Proxies for trade wind changes during Heinrich stadials

– Windblown dust:
    Dust flux and grain size
    Sand dune activity

– Wind-driven coastal upwelling
    SST
    Nutrient supply (e.g., primary productivity, species distribution)

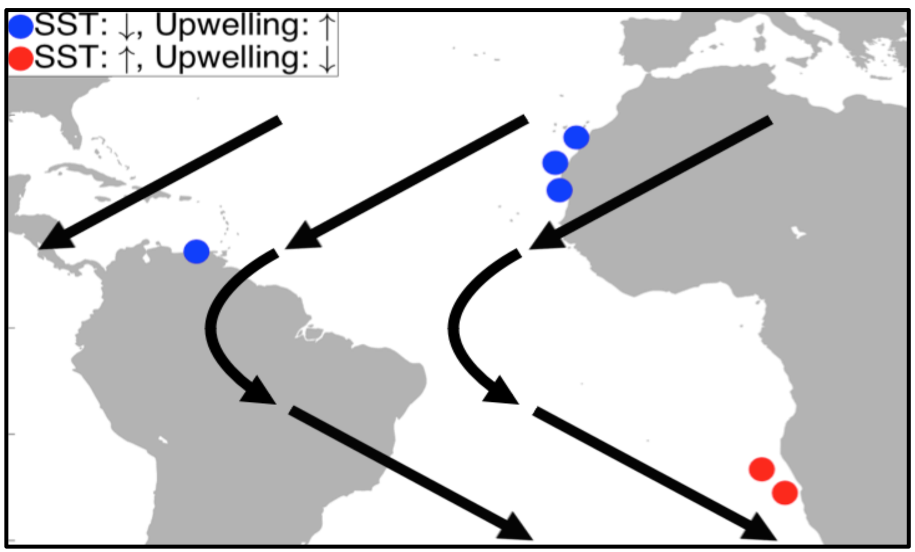

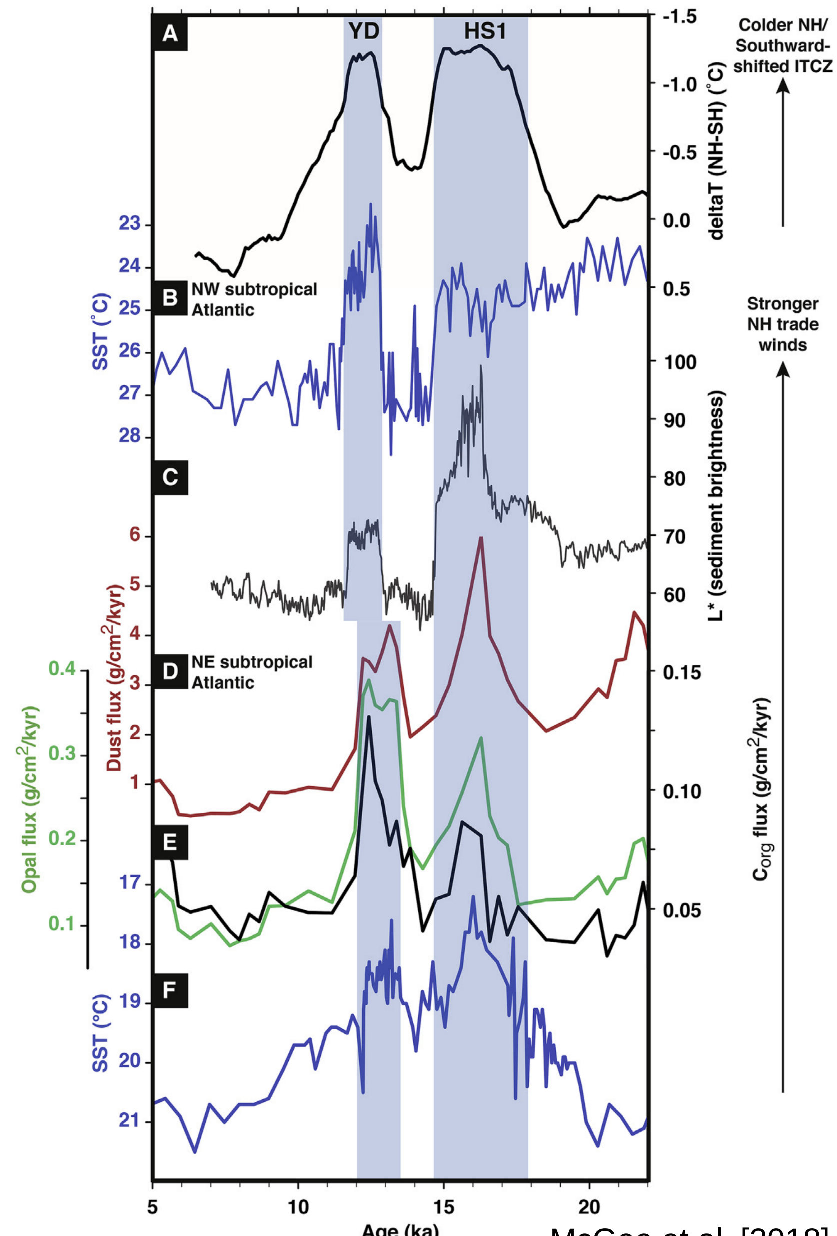

McGee et al. [2018]

Interhemispheric asymmetric trade wind changes in response to a southward ITCZ shift during Heinrich stadials

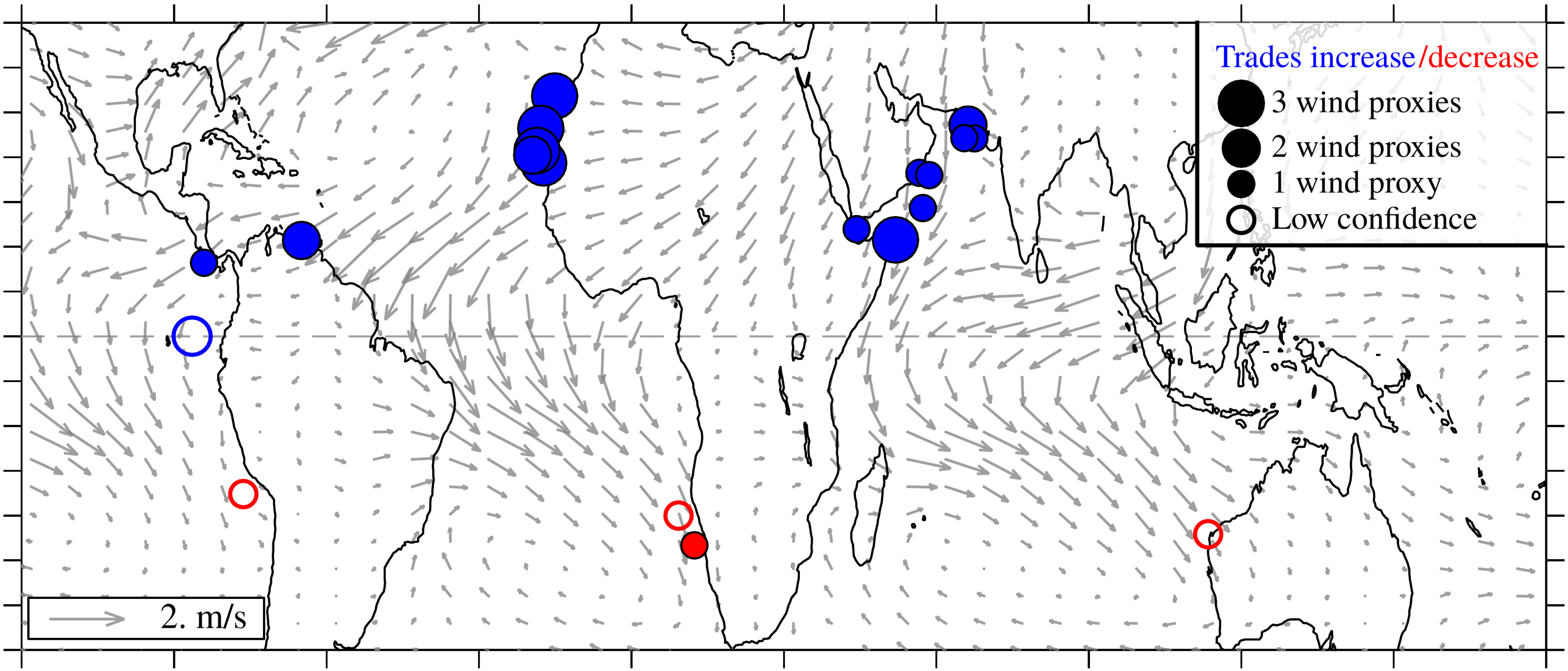

McGee et al. [2018]

Summary: Interhemispheric asymmetric trade wind changes in response to a southward ITCZ shift during Heinrich stadials

– Theory predicts and climate models confirm that a meridional ITCZ shift drives hemispheric asymmetric changes in trade winds

– During Heinrich stadials, proxy evidence of a southward ITCZ shift together with

stronger trade winds in the Northern Hemisphere

weaker trades winds in the Southern Hemisphere

Southward ITCZ shift during cold stadials (weak AMOC or collapse)

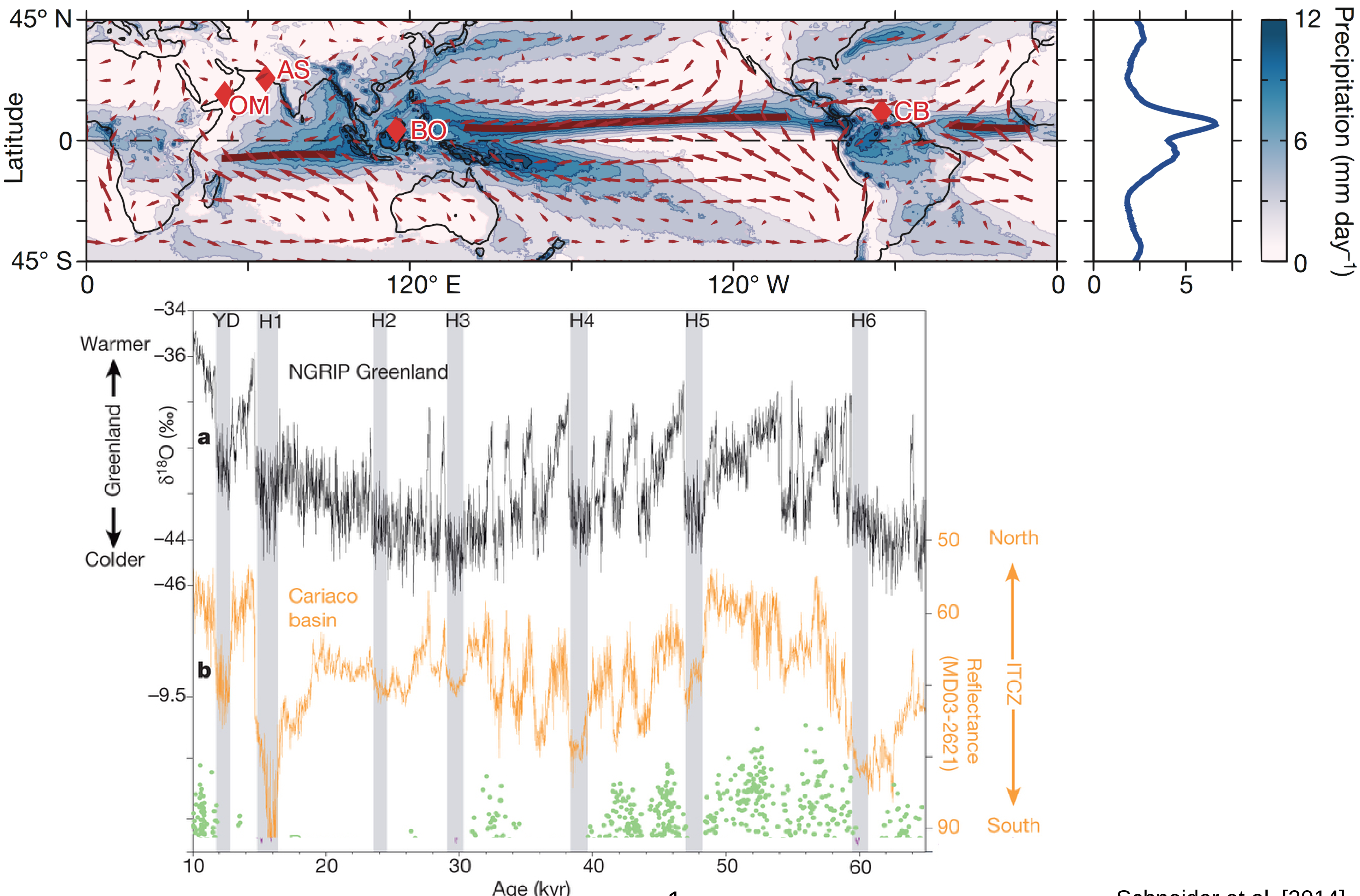

Schneider et al. [2014]

Western US lake expansion in the Great Basin (southwestern US) during Heinrich stadials

What's the physical mechanism behind lake expansions during the Heinrich 1?

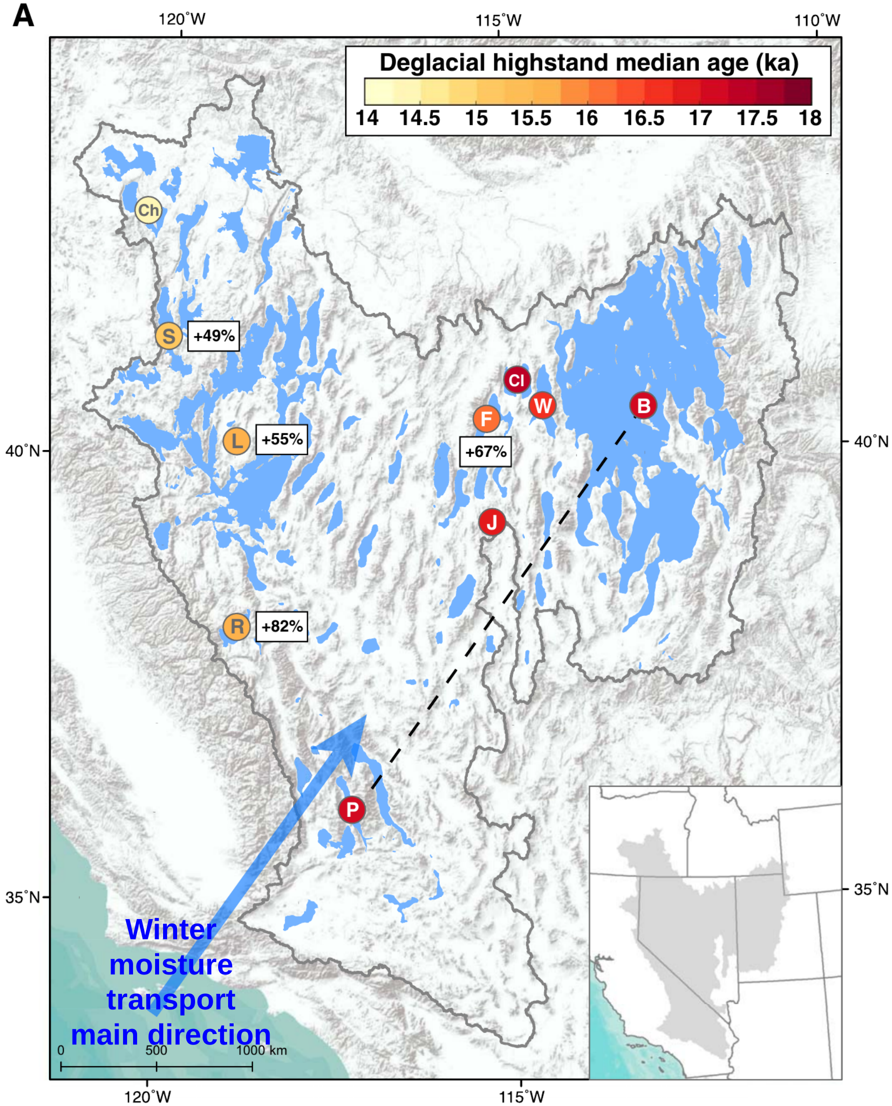

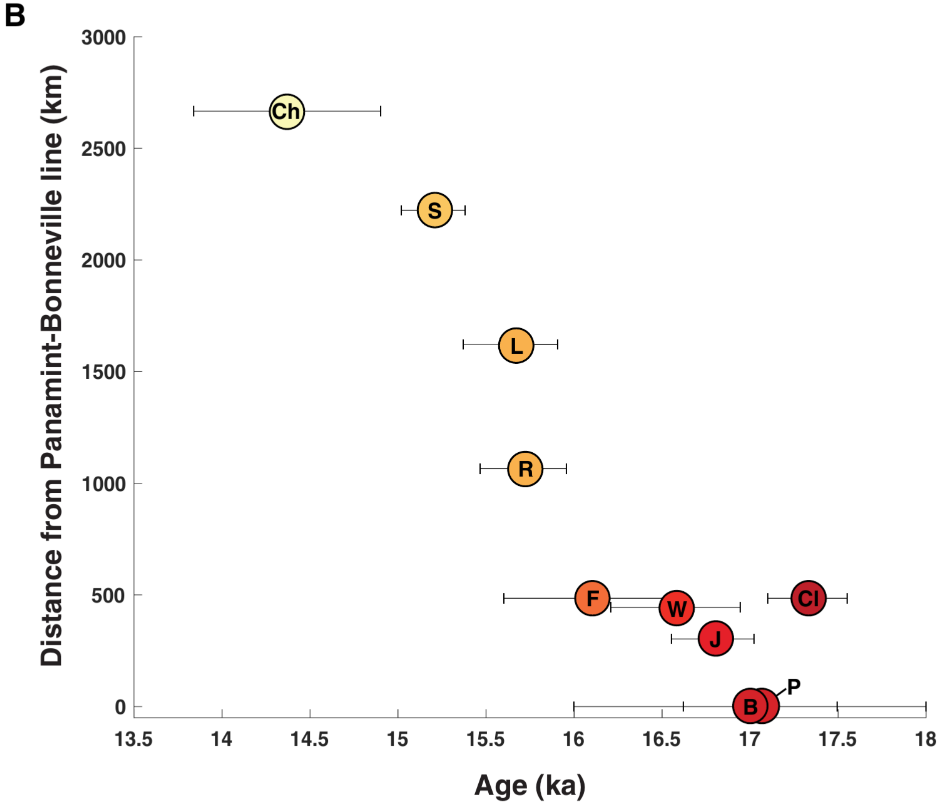

McGee et al. [2019]

Winter precipitation increases in the Great Basin linked to an Aleutian Low deepening

Last-glacial-maximum AMOC collapse simulations with different orbital parameters:

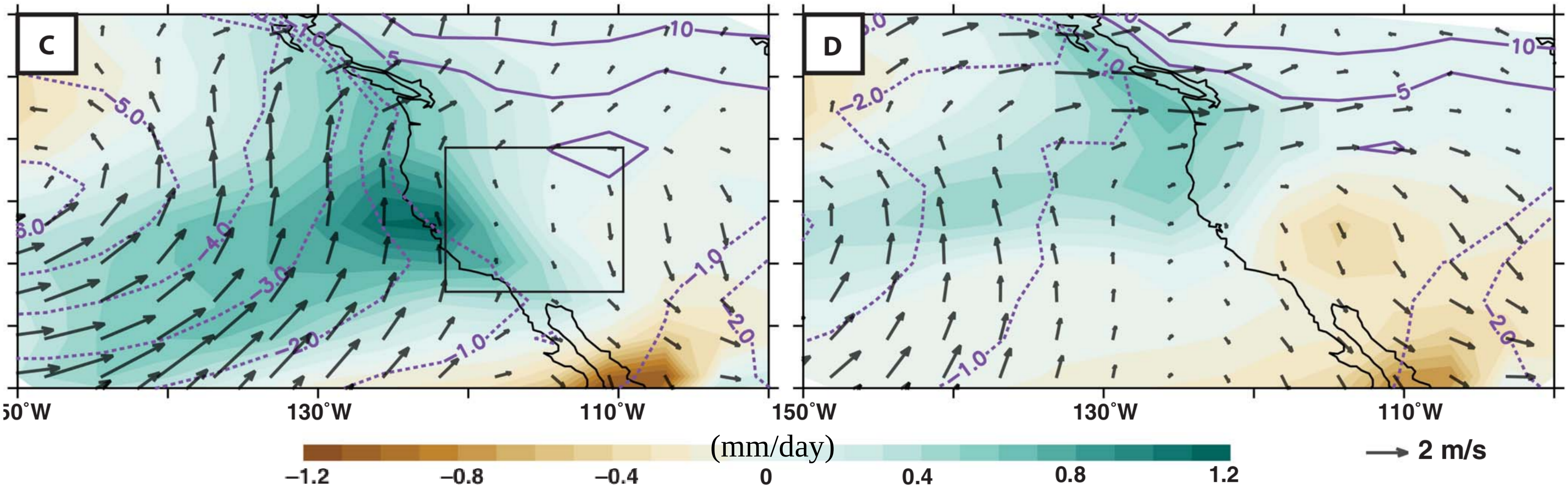

McGee et al. [2019]

Winter precipitation increases in the Great Basin linked to an Aleutian Low deepening

Last-glacial-maximum AMOC collapse simulations with different orbital parameters:

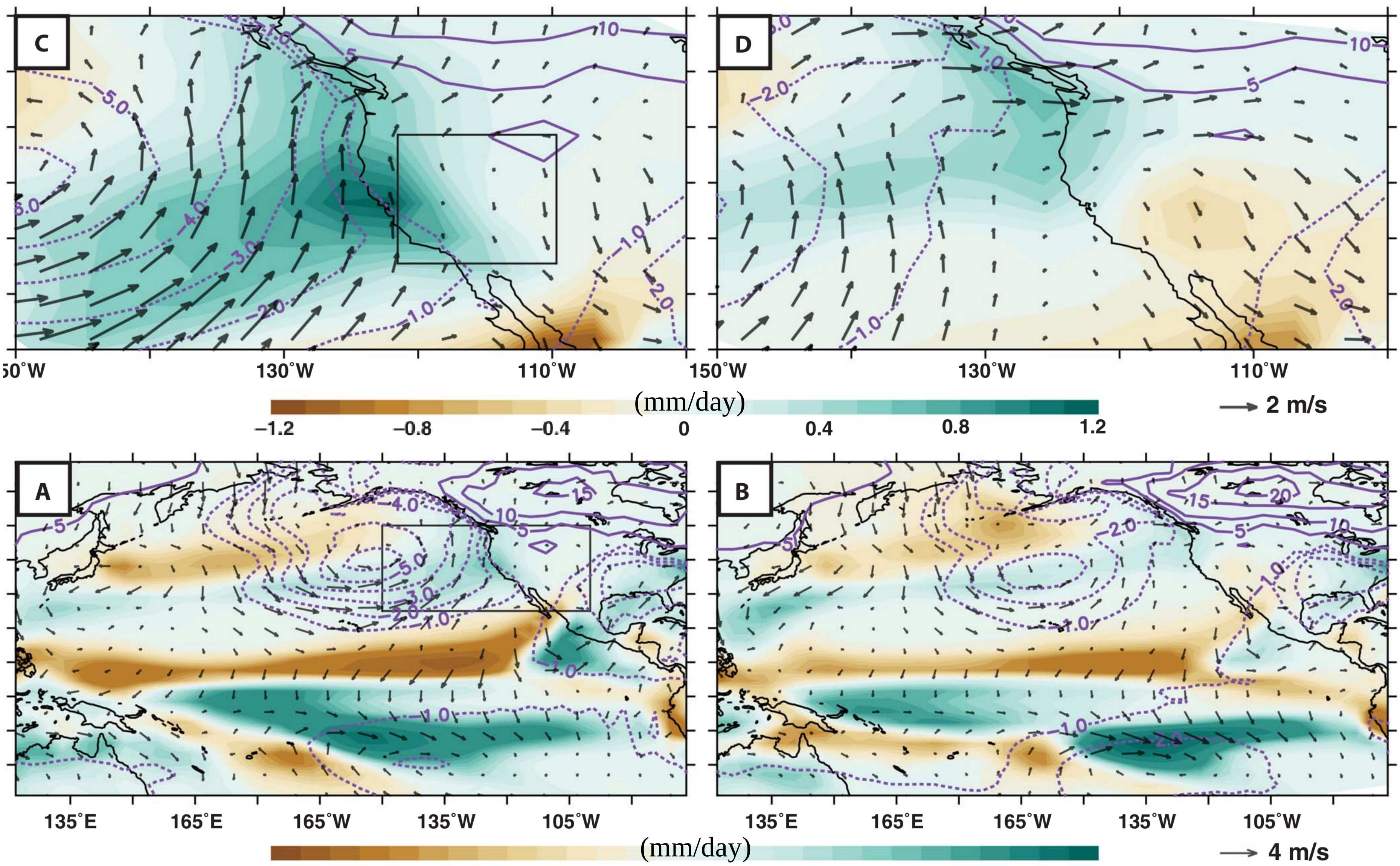

McGee et al. [2019]

Winter precipitation increases in the Great Basin linked to an Aleutian Low deepening, itself linked to a subtropical jet acceleration due to a southward Pacific Hadley cell shift

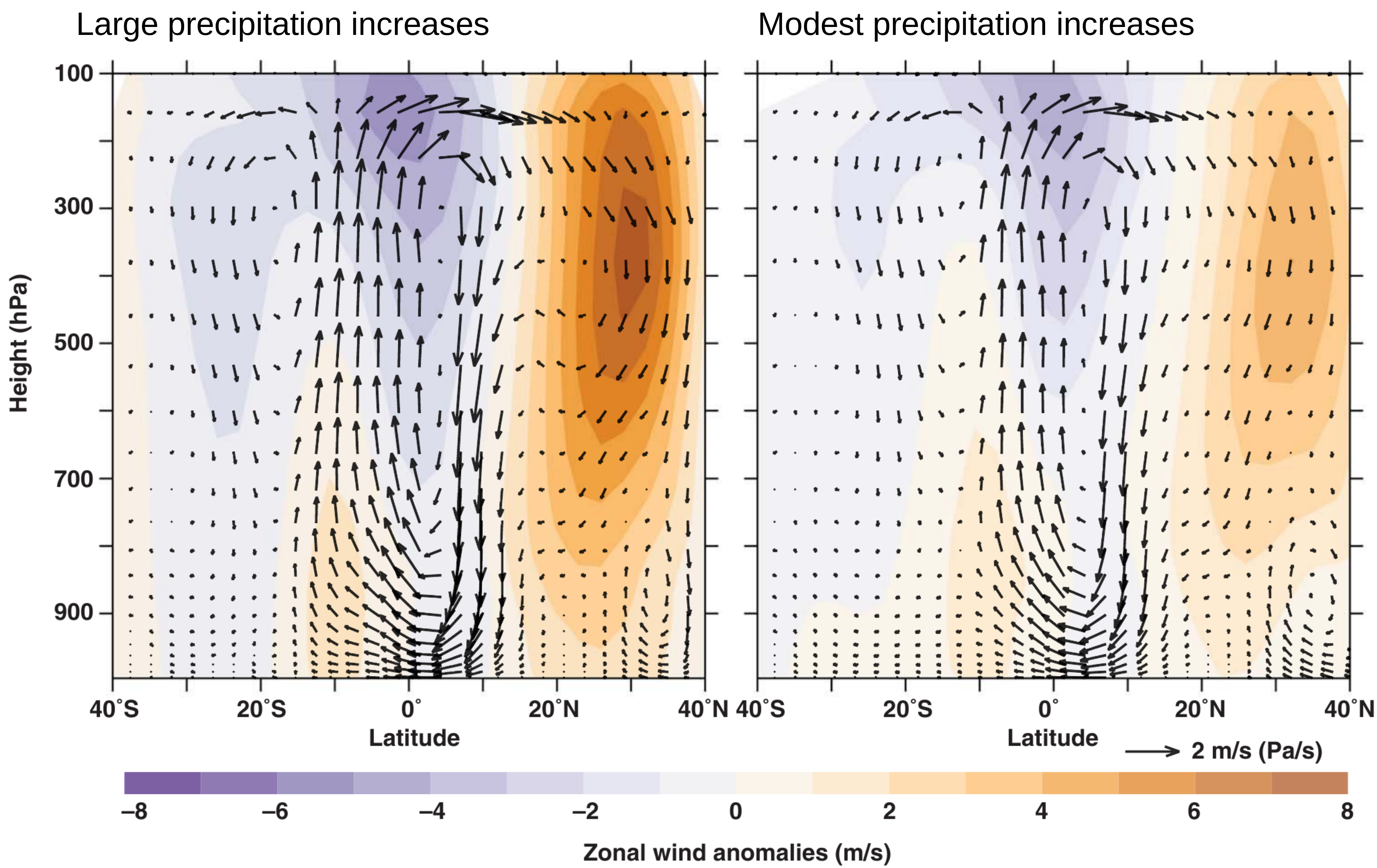

McGee et al. [2019]

Summary: Western US lake expansion linked to Pacific Hadley circulation during Heinrich stadials

– Reconstructed increases in winter precipitation in the Great basin during Heinrich stadials, i.e, North Atlantic and NH cooling

– Precipitation increases driven by subtropical jet intensification and Aleutian Low deepening in response to southward Pacific Hadley cell and ITCZ shift

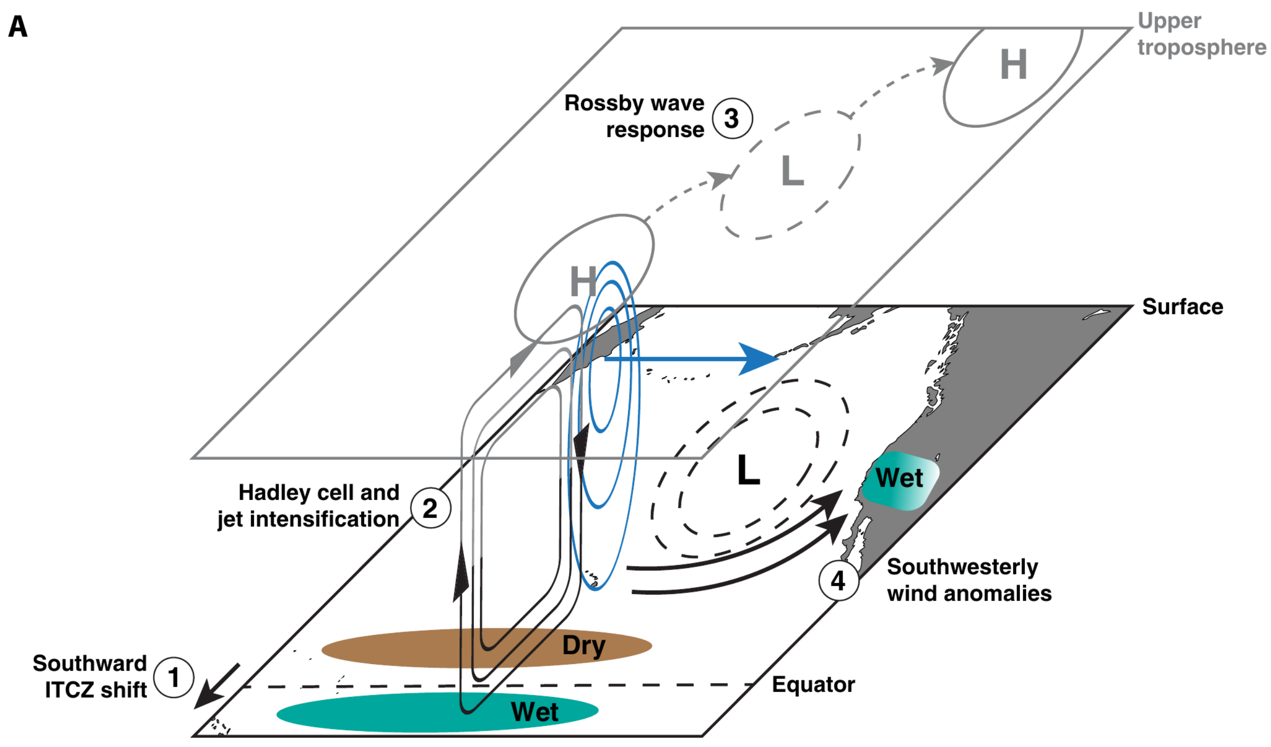

Summary: Exploring linkages between AMOC and ITCZ variability

1. In “modern” climate, simulated AMOC–AMV–ITCZ link, connected to changes in the cross-equatorial heat transport and interhemispheric heating balance

– No similar link with the PDO due to no impact on the interhemispheric energy balance

Summary: Exploring linkages between AMOC and ITCZ variability

1. In “modern” climate, simulated AMOC–AMV–ITCZ link, connected to changes in the cross-equatorial heat transport and interhemispheric heating balance
   – No similar link with the PDO due to no impact on the interhemispheric energy balance

2. In Heinrch stadials, AMOC collapse and North Atlantic cooling driving southward ITCZ and Hadley cell shifts

   – Interhemispheric asymmetric trade wind changes:
   stronger in the NH; weaker in the SH

   – Lake expansions in southwesters US due to winter precipitation increases following a southward Hadley cell shift, subtropical jet acceleration, Aleutian Low deepening

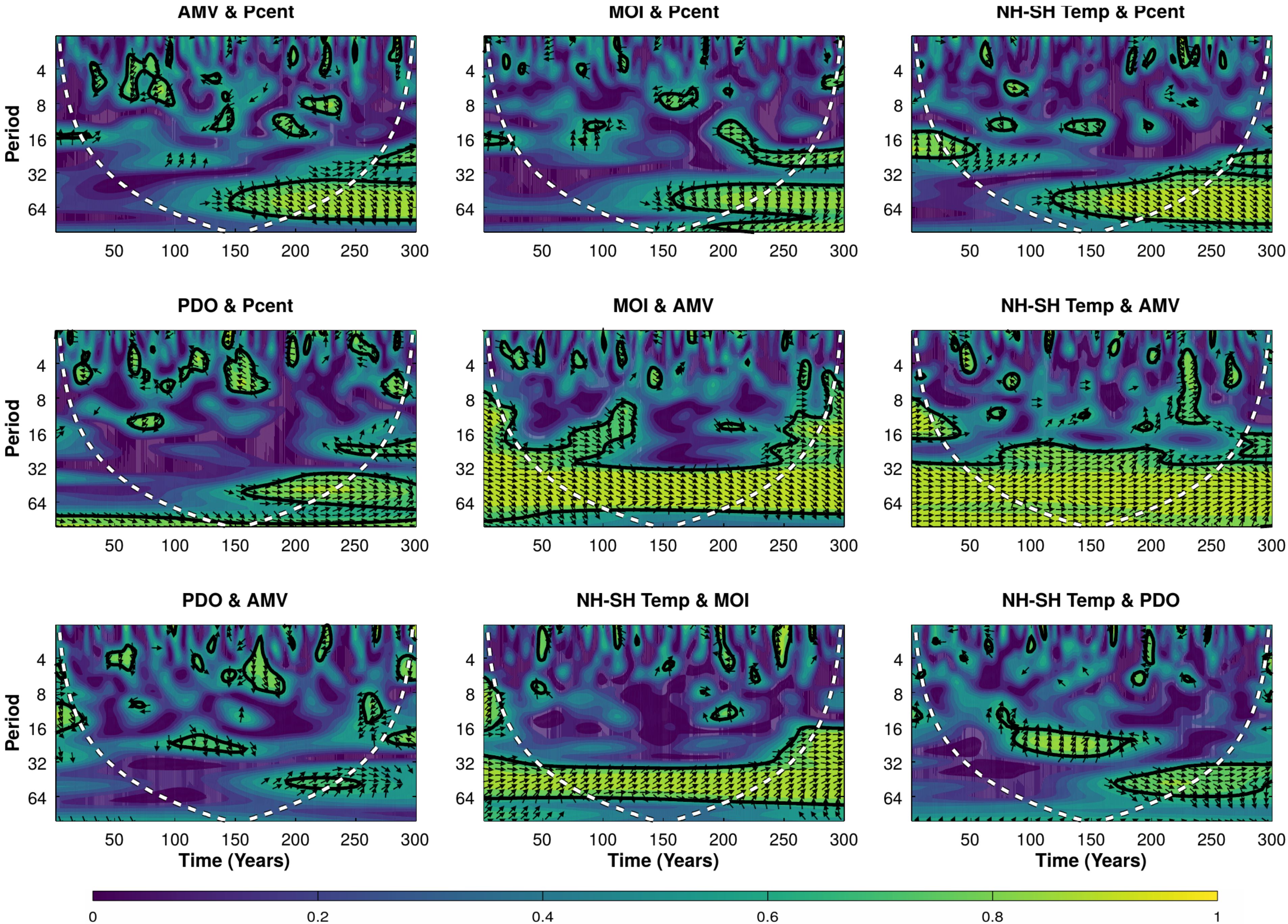

AMV & Pcent
MOI & Pcent
NH-SH Temp & Pcent
PDO & Pcent
MOI & AMV
NH-SH Temp & AMV
PDO & AMV
NH-SH Temp & MOI
NH-SH Temp & PDO
Period
4
8
16
32
64
50
100
150
200
250
300
Time (Years)
0
0.2
0.4
0.6
0.8
1

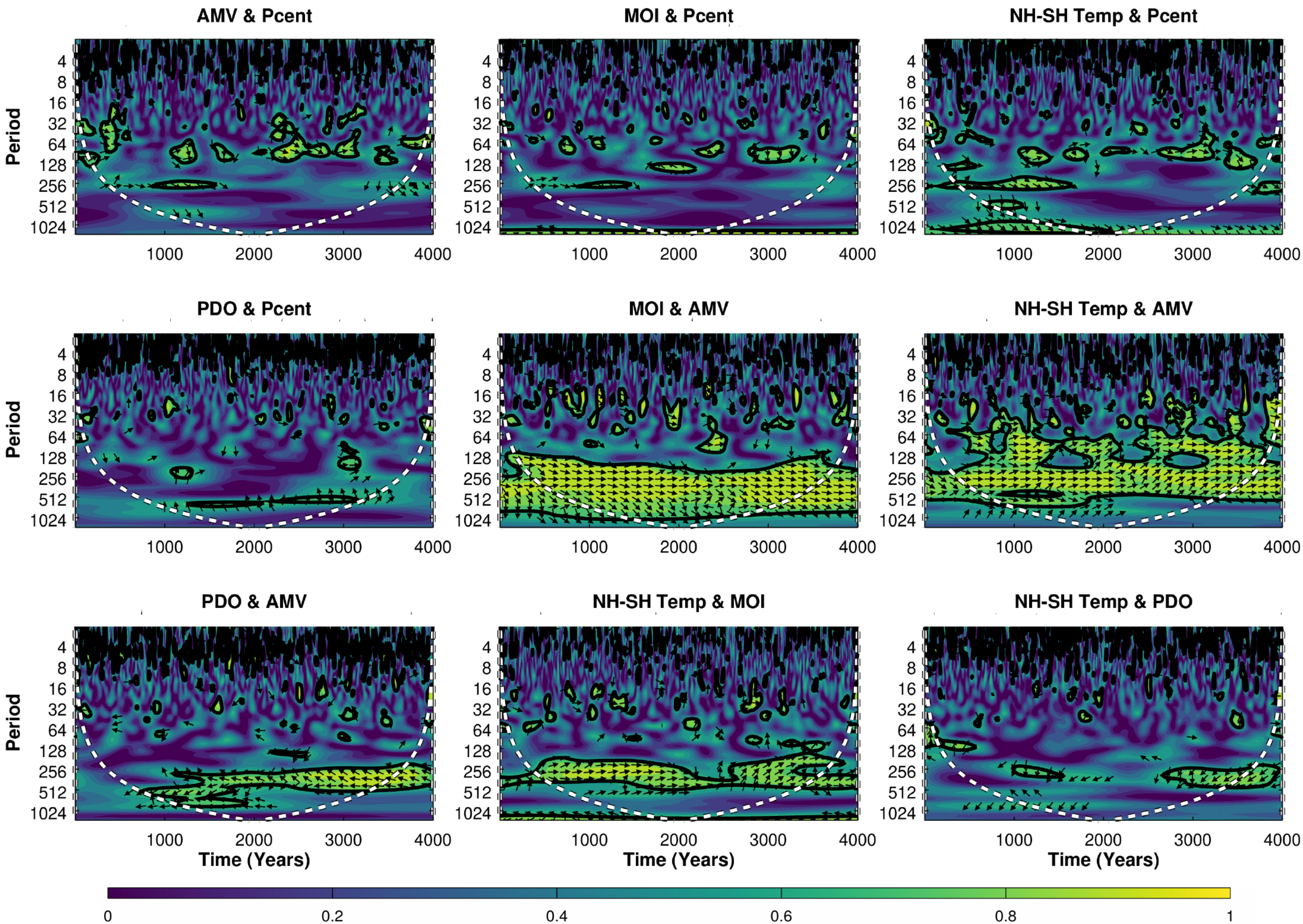
AMV & Pcent
MOI & Pcent
NH-SH Temp & Pcent
PDO & Pcent
MOI & AMV
NH-SH Temp & AMV
PDO & AMV
NH-SH Temp & MOI
NH-SH Temp & PDO
Period
4
8
16
32
64
128
256
512
1024
1000
2000
3000
4000
Time (Years)
0
0.2
0.4
0.6
0.8
1

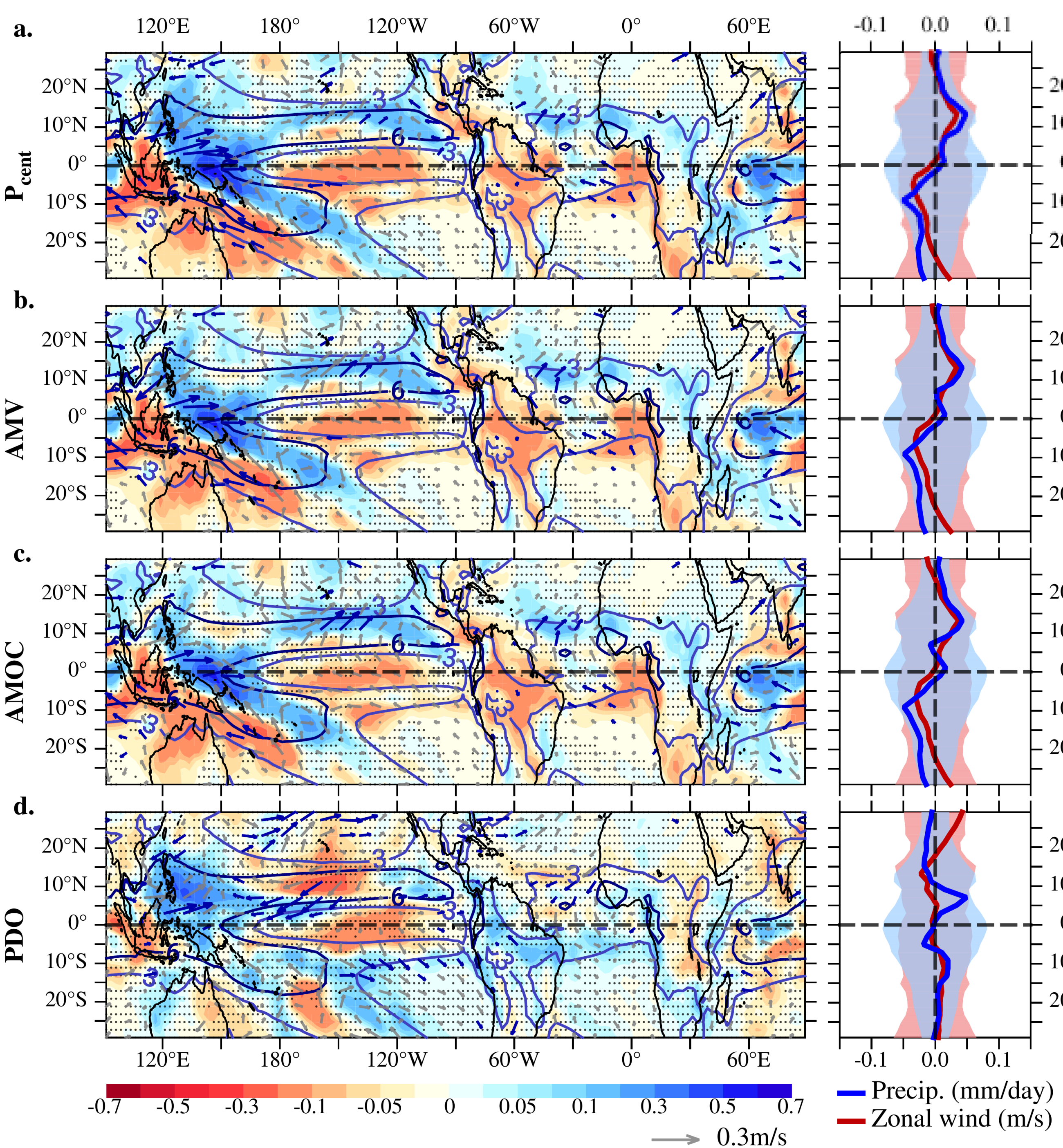

a.
b.
c.
d.
P_cent
AMV
AMOC
PDO
120°E
180°
120°W
60°W
0°
60°E
20°N
10°N
0°
10°S
20°S
-0.1
0.0
0.1
-0.7
-0.5
-0.3
-0.1
-0.05
0
0.05
0.1
0.3
0.5
0.7
0.3m/s
Precip. (mm/day)
Zonal wind (m/s)

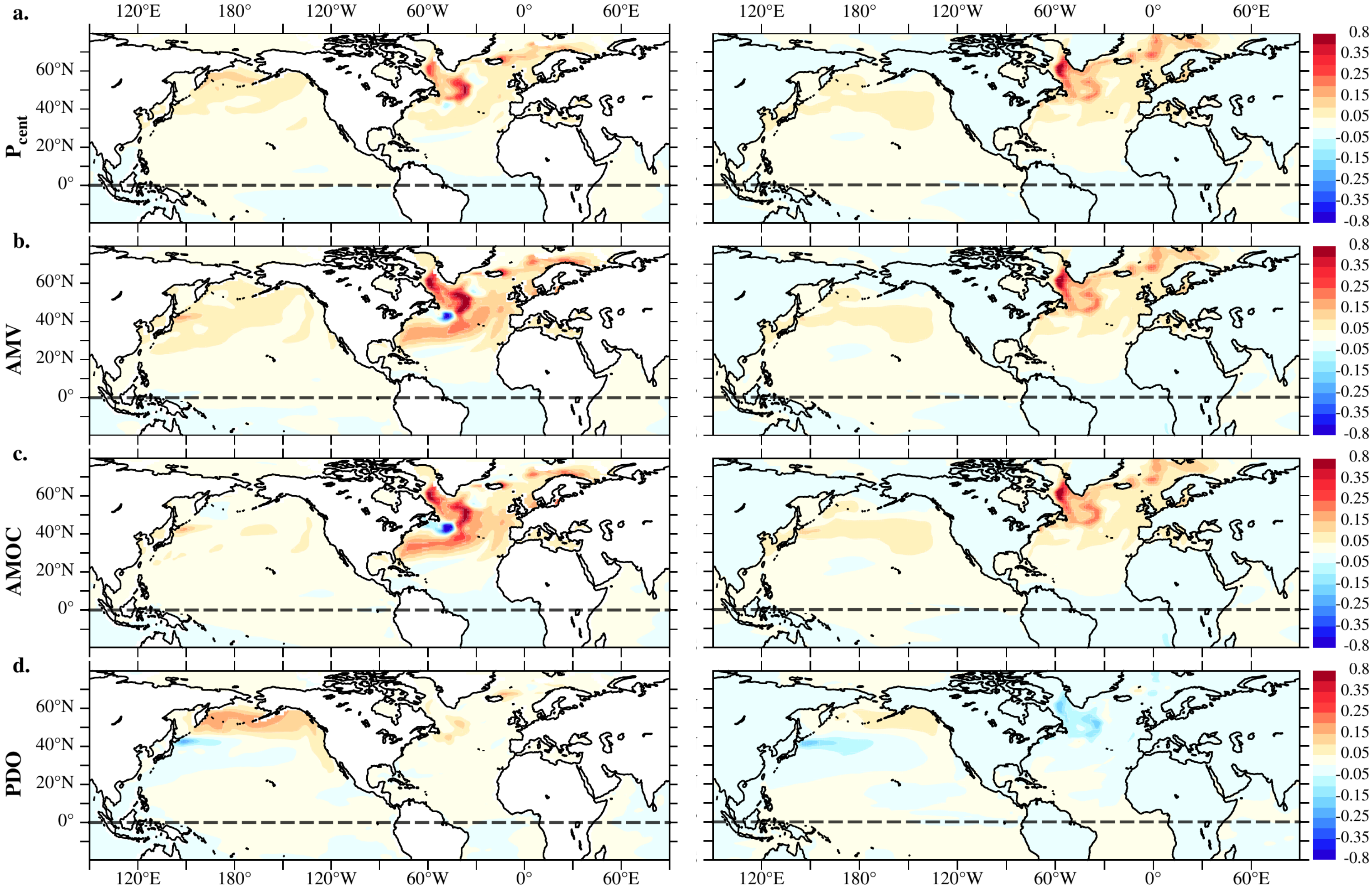

a.
b.
c.
d.
P$_{cent}$
AMV
AMOC
PDO
120°E
180°
120°W
60°W
0°
60°E
60°N
40°N
20°N
0°
0.8
0.35
0.25
0.15
0.05
-0.05
-0.15
-0.25
-0.35
-0.8

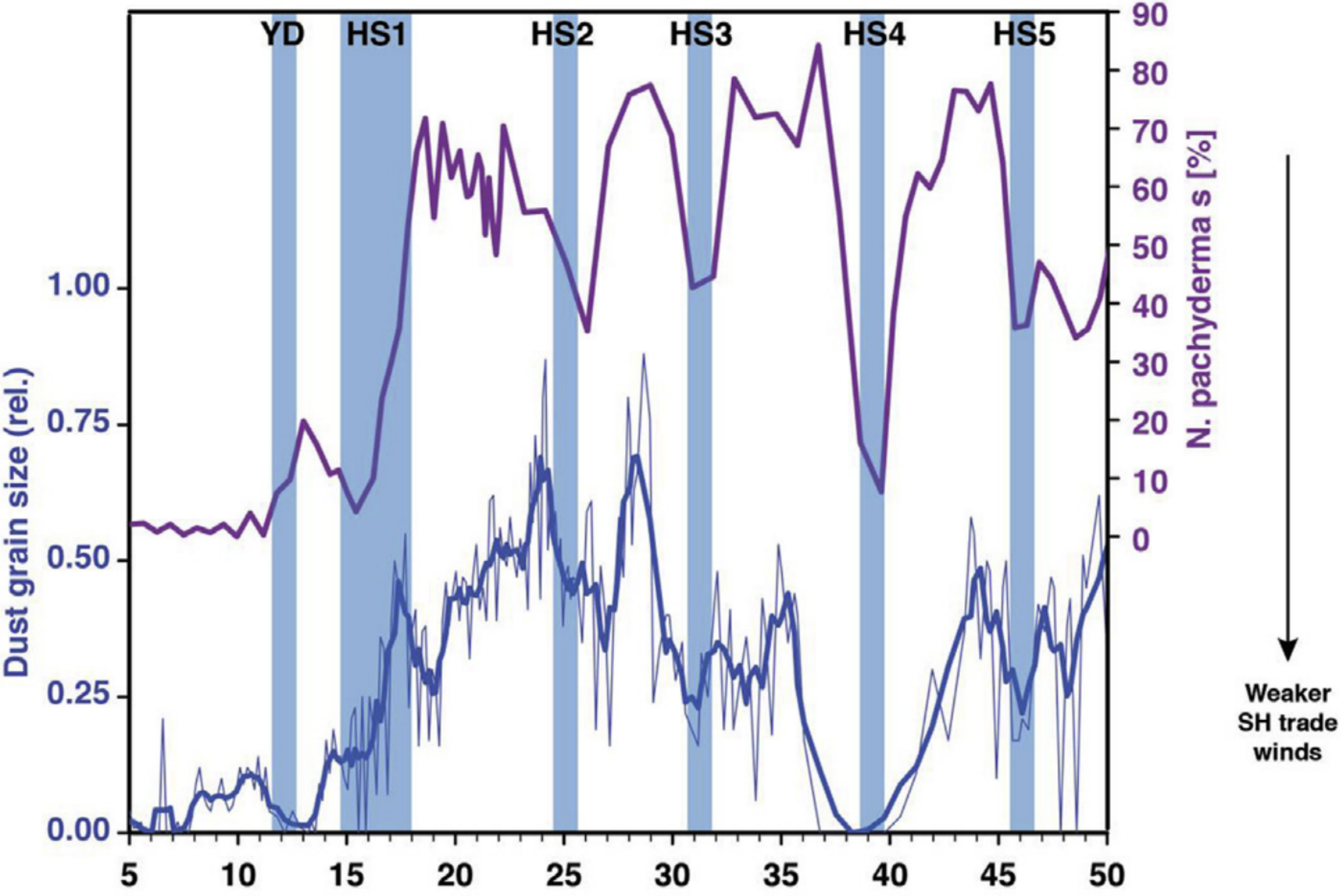
YD
HS1
HS2
HS3
HS4
HS5
Dust grain size (rel.)
0.00
0.25
0.50
0.75
1.00
N. pachyderma s [%]
0
10
20
30
40
50
60
70
80
90
5
10
15
20
25
30
35
40
45
50
Age (ka)
Weaker SH trade winds

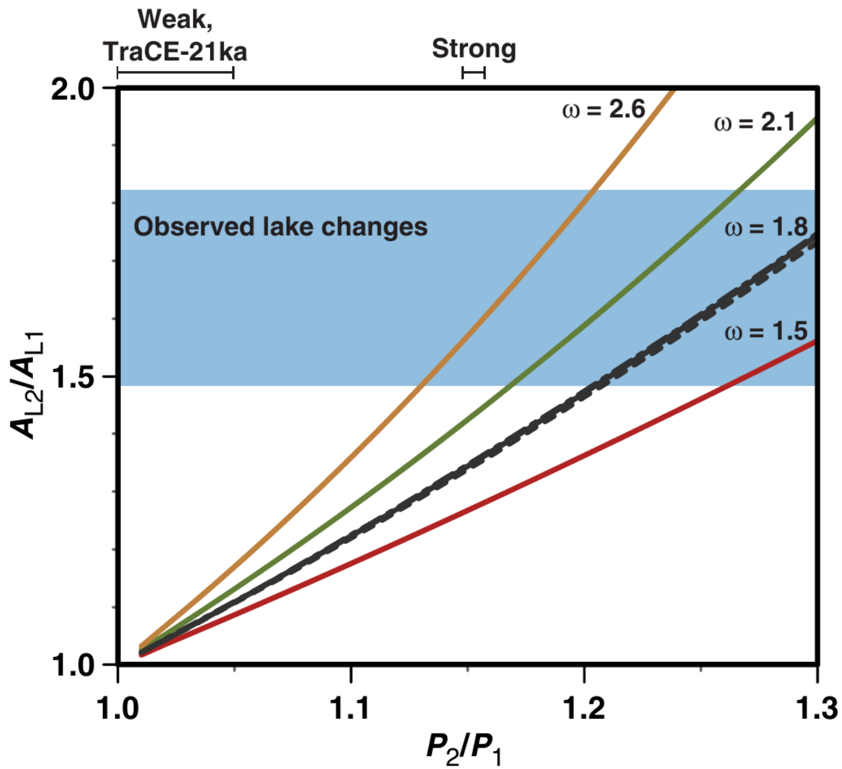

Fig. 3. Simulated lake area changes (A_{L2}/A_{L1}) in response to annual mean precipitation changes (P_2/P_1). Precipitation and lake areas with "1" subscripts represent pre-hosing values, while those with "2" subscripts represent values after hosing. The solid lines correspond to ω values ranging from 1.5 to 2.6, where ω is a basin-specific factor expressing the relationship between precipitation and runoff changes. The value estimated from LGM model simulations (*43*) and our control experiments is 1.8. All solid lines use PET/P_1 = 1.5. The two dashed black lines are calculated for ω = 1.8 and PET/P_1 = 1 and 2; note that there is almost no effect of varying PET/P_1. All lines are calculated assuming no change in PET or E_L and assuming that PET = E_L. Bars at the top indicate precipitation changes in our Strong and Weak hosing simulations and between the LGM and HS1 in the TraCE-21ka experiment. The blue region indicates reconstructed lake area changes between the LGM and HS1 (see the Supplementary Materials).

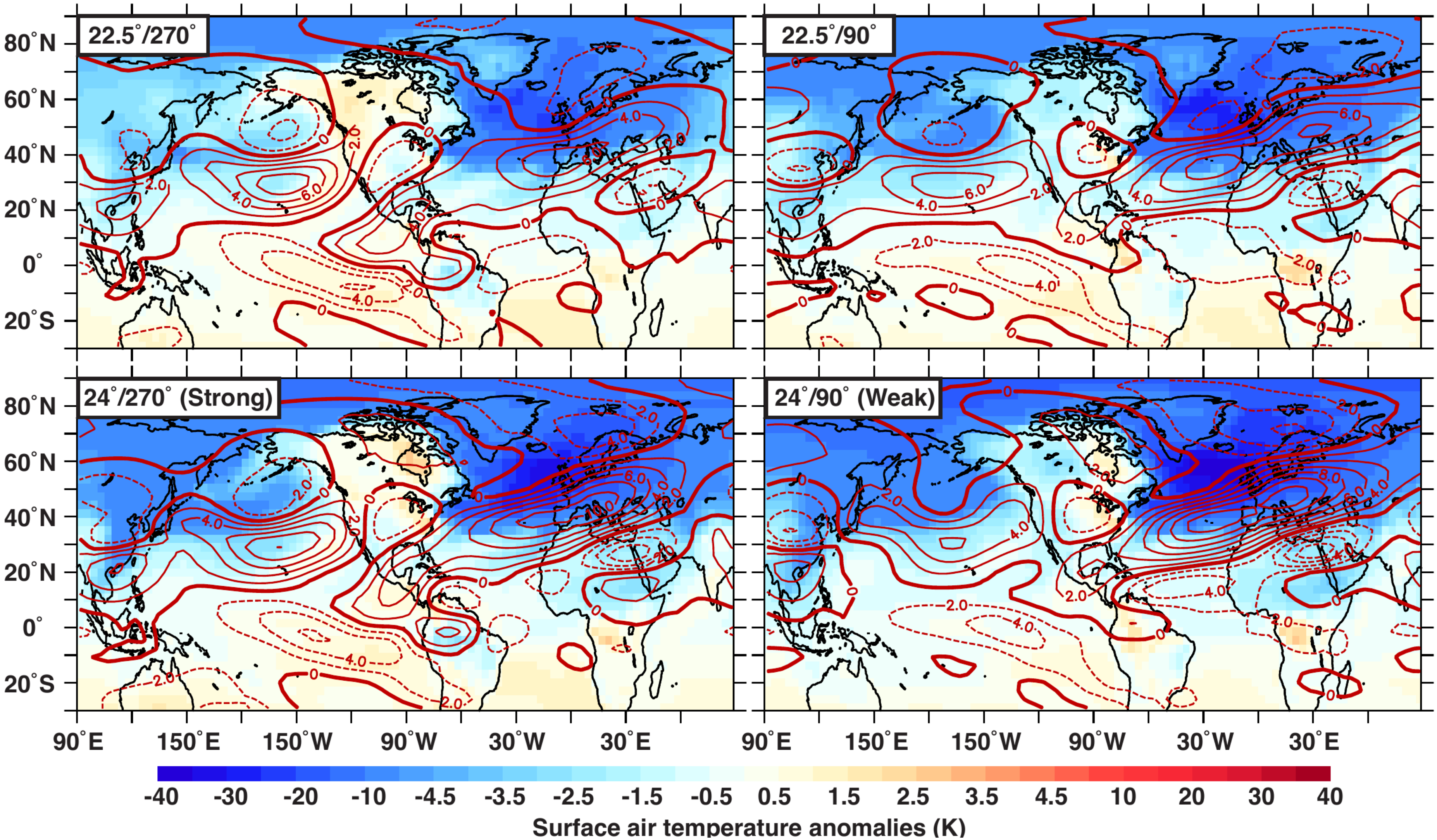

22.5°/270°
22.5°/90°
24°/270° (Strong)
24°/90° (Weak)
80°N
60°N
40°N
20°N
0°
20°S
90°E
150°E
150°W
90°W
30°W
30°E
-40 -30 -20 -10 -4.5 -3.5 -2.5 -1.5 -0.5 0.5 1.5 2.5 3.5 4.5 10 20 30 40
Surface air temperature anomalies (K)

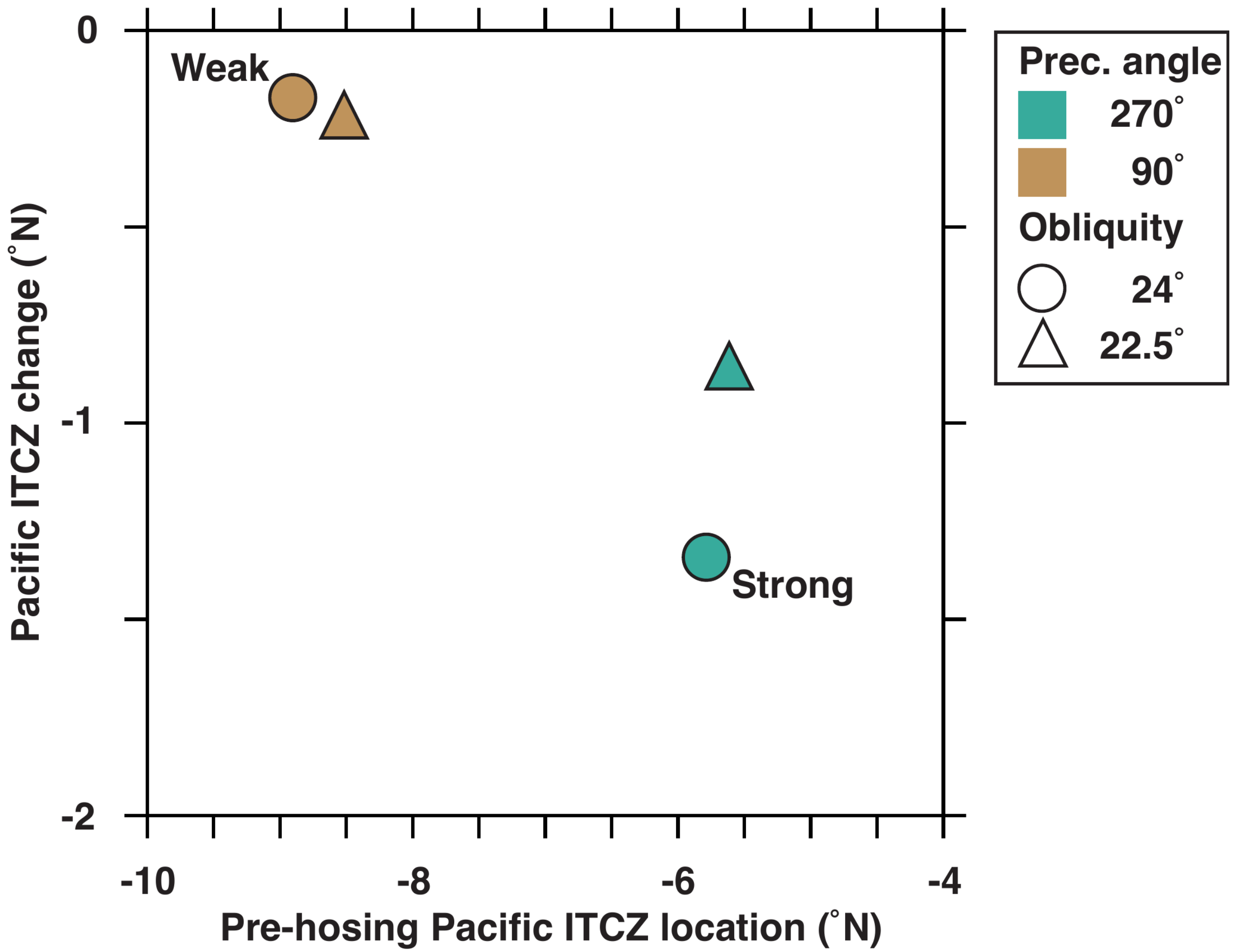

Weak
Strong
Prec. angle
270˚
90˚
Obliquity
24˚
22.5˚
0
-1
-2
-10
-8
-6
-4
Pacific ITCZ change (˚N)
Pre-hosing Pacific ITCZ location (˚N)